

20000831129

AD-A246 334



(2)

THEORETICAL AND EXPERIMENTAL STUDY OF
THERMOACOUSTIC ENGINES

Richard Raspet, Henry E. Bass and W. Pat Arnott
Physical Acoustics Research Laboratory
University of Mississippi
University, Mississippi 38677

DTIC
SELECTE
FEB 25 1992
S D

This document has been approved
for public release and sale; its
distribution is unlimited.



THE UNIVERSITY OF MISSISSIPPI
PHYSICAL ACOUSTICS RESEARCH GROUP
DEPARTMENT OF PHYSICS AND ASTRONOMY

92-04325



19 074

2

THEORETICAL AND EXPERIMENTAL STUDY OF
THERMOACOUSTIC ENGINES

Richard Raspet, Henry E. Bass and W. Pat Arnott
Physical Acoustics Research Laboratory
University of Mississippi
University, Mississippi 38677

ANNUAL REPORT

THE OFFICE OF NAVAL RESEARCH
CONTRACT #N00014-89-J-3087

DTIC
SELECTE
FEB 25 1992
S D D

This document has been approved
for public release and sale; its
distribution is unlimited.

PARGUM REPORT 91-08

DECEMBER, 1991

REPORT DOCUMENTATION PAGE

Form Approved
OMB No 0704-0188

Public reporting burden for this collection of information is estimated to average 1 hour per response, including the time for reviewing existing data sources, gathering and maintaining the data needed, and completing and reviewing the collection of information. Send comments regarding this burden estimate or any other aspect of this collection of information, including suggestions for reducing this burden, to Washington Headquarters Services, Directorate for Information Operations and Reports, 1215 Jefferson Davis Highway, Suite 1204, Arlington, VA 22202-4302, and to the Office of Management and Budget, Paperwork Reduction Project (0704-0188), Washington, DC 20503.

1. AGENCY USE ONLY (Leave blank)		2. REPORT DATE 31 Dec 91		3. REPORT TYPE AND DATES COVERED Annual 01 Jan 91 - 31 Dec 91	
4. TITLE AND SUBTITLE Theoretical and Experimental Study of Thermoacoustics Engines				5. FUNDING NUMBERS PE 61153N11 G N00014-89-J-3087 TA uri5005	
5. AUTHOR(S) Richard Rapset, Henry E. Bass and W. Pat Arnott					
7. PERFORMING ORGANIZATION NAME(S) AND ADDRESS(ES) Physical Acoustics Research Laboratory University of Mississippi University, MS 38677				8. PERFORMING ORGANIZATION REPORT NUMBER PARGUM 91-08	
9. SPONSORING/MONITORING AGENCY NAME(S) AND ADDRESS(ES) Office of Naval Research Physics Division - Code 1112 800 North Quincy Street Arlington, VA 22217-5000				10. SPONSORING/MONITORING AGENCY REPORT NUMBER	
11. SUPPLEMENTARY NOTES					
12a. DISTRIBUTION/AVAILABILITY STATEMENT Approved for public release; Distribution unlimited				12b. DISTRIBUTION CODE	
13. ABSTRACT (Maximum 200 words) Thermoacoustic engines can be used to pump heat using a sound wave (refrigerator or heat pump) or pump a sound wave using a temperature gradient (prime mover). The basic arrangement is a gas-filled acoustic resonator with appropriately positioned thermoacoustic elements. Two types of thermoacoustic elements are used in these engines. The first type are heat exchangers which are used to communicate heat between the gas and external heat reservoirs. The second type is the thermoacoustic engine (TAE), also known as a stack. The TAEs are sections of porous media that support the temperature gradient, that transport heat on the acoustic wave between the exchangers, and that produces or absorbs acoustic power. Previous theoretical results in thermoacoustics have been developed for TAEs with circular or parallel slit pore geometries. We have developed a general linear formulation for gas-filled TAEs having pores of arbitrary cross-sectional geometry. This analysis, which is very helpful in designing optimal engines, indicates the parallel slit pore geometry optimizes heat and work flow. Included are an introductory section where fundamentals of thermoacoustics are briefly discussed, a summary of our theoretical analysis, acoustical measurements of an air-filled thermoacoustic prime mover, and numerical results for a recently constructed helium-filled prime mover.					
14. SUBJECT TERMS thermoacoustics, acoustic source				15. NUMBER OF PAGES 61	
				16. PRICE CODE	
17. SECURITY CLASSIFICATION OF REPORT UNCLASSIFIED	18. SECURITY CLASSIFICATION OF THIS PAGE UNCLASSIFIED	19. SECURITY CLASSIFICATION OF ABSTRACT UNCLASSIFIED	20. LIMITATION OF ABSTRACT		

TABLE OF CONTENTS

	Page
Abstract	1
Introduction.	1
Thermoacoustics in the Lagrangian and Eularian Fluid Frames.	4
Specific Acoustic Impedance and Pressure Translation Theorems	9
Heat and Work Flow in the Short Stack Approximation for Various Stack Geometries	11
Demonstration Air-Filled Thermoacoustic Prime Mover.	14
Numerical Results for a Helium-Filled Prime Mover	17
General Prime Mover Analysis Using Energy Boundary Conditions	20
Sundry Remarks	21
References.	23
Publications and Presentations.	23
Appendix: FORTRAN Program for Analysis of the UM TAE	27
Figures.	47

Accession For	
NTIS CRA&I	<input checked="" type="checkbox"/>
DTIC TAB	<input type="checkbox"/>
Unannounced	<input type="checkbox"/>
Justification	
By	
Distribution /	
Availability Codes	
Dist	Avail and/or Special
A-1	



ANNUAL REPORT ON THEORETICAL AND EXPERIMENTAL STUDY OF THERMOACOUSTIC ENGINES

Richard Raspet, Henry E. Bass, and W. Pat Arnott
Physical Acoustics Research Laboratory
University of Mississippi
University, Mississippi, 38677

ABSTRACT

Thermoacoustic engines can be used to pump heat using a sound wave (refrigerator or heat pump) or pump a sound wave using a temperature gradient (prime mover). The basic arrangement is a gas-filled acoustic resonator with appropriately positioned thermoacoustic elements. Two types of thermoacoustic elements are used in these engines. The first type are heat exchangers which are used to communicate heat between the gas and external heat reservoirs. The second type is the thermoacoustic engine (TAE), also known as a stack. The TAEs are sections of porous media that support the temperature gradient, that transport heat on the acoustic wave between the exchangers, and that produce or absorb acoustic power. Previous theoretical results in thermoacoustics have been developed for TAEs with circular or parallel slit pore geometries. We have developed a general linear formulation for gas-filled TAEs having pores of arbitrary cross-sectional geometry. This analysis, which is very helpful in designing optimal engines, indicates the parallel slit pore geometry optimizes heat and work flow. Included are an introductory section where fundamentals of thermoacoustics are briefly discussed, a summary of our theoretical analysis, acoustical measurements of an air-filled thermoacoustic prime mover, and numerical results for a recently constructed helium-filled prime mover.

INTRODUCTION

Thermoacoustics is broadly classified as the interaction of heat and sound. The branch of thermoacoustics we consider is heat driven oscillations of gas in a tube and thermoacoustic transport of heat. The basic arrangement is shown in Fig. 1a where thermoacoustic elements of

heat exchangers and a TAE are shown in the gas-filled driven resonance tube. The plane wave mode of the resonator is considered to be dominant and pressure and particle velocity have near standing-wave phasing. This arrangement could be used to deliver acoustic power to the TAE for heat transport from cold to hot (for low temperature gradients $(T_H - T_C)/d$) as in a normal refrigerator. Thermoacoustic elements are sections of capillary-tube-type porous media as shown in Fig. 1b. Theory for the system is built from the model for sound in a single arbitrary-perimeter capillary tube as shown in Fig. 1c. Some pore perimeter shapes which have been considered are shown in Fig. 2. Single tube radii are usually designed to equal the frequency-dependent thermal boundary layer thickness δ_T for optimal performance. By removing the acoustic driver and supplying a sufficiently high temperature gradient, the TAE produces acoustic power at the resonant frequency of the system.

Observations of heat-driven acoustic oscillations date back to at least the eighteenth century. Rayleigh¹ gave a qualitative explanation well-worth quoting: "In almost all cases where heat is communicated to a body, expansion ensues, and this expansion may be made to do mechanical work. If the phases of the forces thus operative be favorable, a vibration may be maintained." Acoustic oscillations were noted to frequently occur in a capillary tube filled with helium vapor with one end of the tube at approximately 2 K and the other at room temperature and a qualitative explanation similar to Rayleigh's was given.² A full, linear, theoretical investigation of heat-driven acoustic oscillations was performed first by N. Rott³ and was explored in a series of papers starting in 1969. Rott has reviewed this work.⁴

The reciprocal mode of operation, which uses a sound wave in a resonator to transport heat from cold to hot as in a refrigerator, has also been of recent interest. This thermoacoustic streaming has its analogy in acoustic streaming, which is the transport of mass by an acoustic wave.⁵ Merkli and Thomann⁶ found experimental verification for their theory of thermoacoustic streaming in a driven resonance tube. Wheatley, Swift, Hofler, Garrett and others have developed the notion that the arrangement shown in Fig. 1a can be viewed as a thermodynamic heat engine.^{7,8} Swift has expertly reviewed this work.⁹ The thermodynamic heat engine point of view

enhances the understanding of thermoacoustics and is very helpful in evaluating practical devices. The connection between Refs. 4, 6, and 9 has been briefly explored by Rott.¹⁰ Other references to the early history and practitioners of thermoacoustics can be found in the review articles.^{4,9}

A common approach for the theory of sound in porous media is to envision the medium as a collection of circular capillary tubes.¹¹ The generalization to capillary tubes of arbitrary geometry has recently been explored.¹² The equations and boundary conditions used in porous media modeling and in thermoacoustics are nearly identical (thermoacoustics has an extra term proportional to the ambient temperature gradient that occurs when evaluating the time rate of change of the entropy). It was apparent to us that thermoacoustic theory should be cast in a sufficiently simple form that analysis of pore geometries other than circles⁴ and parallel slits^{4,9} would be readily possible.

In particular, we have considered use of extruded ceramic monolithic catalyst supports (for example, the ceramic used in some automobile catalytic converters) for use in thermoacoustics on account of their low thermal conductivity and regular square-pore geometry.¹³ This material has main pores of diameter 1.54 mm. In addition, the walls of the main pores are porous as well, with typical wall pores of diameter 25 μm . The frequency-dependent complex propagation constant of sound in the square pore ceramic was measured in related work.¹⁴ The specific acoustic impedance of a 49 cm long piece was measured both before and after the wall pores were filled. These measurements verified our theory for sound propagation in porous wall porous media.¹⁵ The TAE used in the lecture demonstration was a sample of this ceramic.

We have extended thermoacoustic theory to include the acoustic field quantities and the second order energy flow for arbitrary perimeter pores.¹⁶ Heat and work flow were compared in the short stack approximation to investigate the effects of pore geometry. Once the acoustical properties of the separate thermoacoustic elements have been determined the elements must be connected in series inside of a resonator as shown in Fig. 1a. Numerical integration of the acoustical equations is used to compute field quantities in the stack since in general a temperature gradient exists from one end to the other.^{4,9} The physical parameters of ambient density,

viscosity, sound speed, thermal conductivity, etc, are temperature dependent and thus depend on location within the TAE. Specific acoustic impedance and pressure translation theorems were developed¹⁶ to compute all acoustical field quantities and energy flow at each point in the resonance tube shown in Fig. 1a.

THERMOACOUSTICS IN THE LAGRANGIAN AND EULARIAN FLUID FRAMES

Figure 3a and 3b depict an inviscid gas parcel oscillating between solid parallel plates at the extremes of motion in the Lagrangian frame. Heat transfer can usually be neglected in normal low frequency acoustics. However, for parcels near solid surfaces heat exchange is likely to occur. Standing wave phasing is assumed so fluid parcel displacement and pressure are in phase. The plates have a temperature gradient along them in the direction of oscillation. The location for wall temperature T_0 is nominally the parcel equilibrium location. The magnitude of the temperature gradient determines whether heat is transferred to or from the gas parcel. The right end of the plate faces a pressure antinode and the left end a pressure node. Consider first the heat pump operation in Fig. 3a. The gas parcel is rapidly displaced left a distance d from equilibrium. During displacement parcel pressure and hence temperature diminishes and expansion occurs. At the leftmost location, the parcel is momentarily still so the possibility of (slow) heat transfer from the wall occurs. For a small wall temperature gradient, the parcel is now at a lower temperature than the wall so heat flows from the wall to the parcel. After transfer of heat dQ' from the wall to the parcel, the parcel expands to the size shown by the shaded square and work is done by the parcel on the gas to the left. This work discourages vibration of the gas to the left since that gas is in the expansion part of the cycle. The parcel then is displaced to the right a distance $2d$. Heat dQ is transferred to the wall from the parcel, and the parcel shrinks to the size shown by the shaded square. The parcel absorbs work from the gas to the right which is in the compressional part of the acoustic cycle. Net heat is transported by the parcel from the wall at temperature $T_0 - \Delta T$ to the wall at temperature $T_0 + \Delta T$. It is now easy to see that heat from an exchanger at the left can be

transported up the temperature gradient to a heat exchanger on the right and that acoustic power is absorbed by the parcel.

Consider next the prime mover in Fig. 3b. The gas parcel is rapidly displaced left a distance d from equilibrium. For a large wall temperature gradient, the parcel is now at a higher temperature than the wall so heat flows from the parcel to the wall. After transfer of heat dQ' from the parcel to the wall, the parcel shrinks to the size shown by the shaded square and work is absorbed by the parcel. This work encourages vibration of the gas to the left since that gas is in the expansion part of the cycle. The parcel then is displaced to the right a distance $2d$. Heat dQ is transferred to the parcel from the wall, and the parcel enlarges to the size shown by the shaded square. The parcel delivers work to the gas on the right which is in the compressional part of the acoustic cycle, thus encouraging vibration. Net heat is transported by the parcel from the wall at temperature $T_0 + \Delta T$ to the wall at temperature $T_0 - \Delta T$. It is now easy to see that heat from an exchanger at the right can be transported down the temperature gradient to a heat exchanger on the left and that acoustic power is produced by the parcel.

Figure 4 shows the temperature disturbance for $\Delta T=0$ at a fixed coordinate system (Eularian frame) with y -axis as shown in Fig. 3b. The excess (or acoustic) temperature changes due to pressure changes of the gas and conduction of heat to the walls. The assumed boundary condition for $Y=\pm 1$ is that fluid and wall temperature are the same. The quantity shown is $T(y)/T_{ad} = F(Y, \lambda_T) = 1 - \cosh[(-i)^{1/2} \lambda_T Y / 2] / \cosh[(-i)^{1/2} \lambda_T / 2]$, where $Y = y/(2a)$ is a normalized coordinate, $\lambda_T = 2a (\rho_0 \omega c_p / \kappa)^{1/2} = 2^{3/2} a / \delta_\kappa$ is a normalized number proportional to the ratio of the plate spacing $2a$ and thermal boundary layer thickness δ_κ ; ρ_0 , c_p , and κ are the gas ambient density, isobaric heat capacity per unit mass, and thermal conductivity; and ω is the radian frequency.¹⁶ The case shown has $\lambda_T = 3.2$. The quantity $T_{ad} = (\gamma - 1) P_1 / (\beta \rho_0 c^2)$ is the acoustic temperature (driven by the acoustic pressure P_1) that would occur in the gas if no heat transfer occurred as in normal adiabatic oscillation of sound waves (γ is C_p/C_v , β is the coefficient of thermal expansion, and c is the adiabatic sound speed). The magnitude of the excess gas temperature nearly reaches the adiabatic sound value at $Y = 0$, and diminishes to zero at the gas-

solid boundary. The phase difference between excess temperature and pressure occurs because as the pressure increases, excess temperature increases, and particle velocity decreases (on account of standing wave phasing), heat is transferred to the wall, cooling the gas. The excess temperature is a maximum at a time between maximum particle velocity and maximum pressure at a given location. This time phasing between motion and heating is a common feature of heat engines. The excess temperature for non-zero ΔT is modified by convective transport of gas and by gas viscosity.¹⁶ Analysis for the heat transferred into the wall when $\Delta T = 0$ has been done.⁶

Consider the single pore shown in Fig. 1c. Denote the first order acoustic variables as follows: $v(x,y,z) = v_x(x,y,z) + v_z(x,y,z)\hat{z}$ is particle velocity, $P_1(z)$ is pressure, $\rho_1(x,y,z)$ is density, and $T_1(x,y,z)$ is temperature. Ambient quantities are indicated by subscript 0. The linearized fluid equations for constant frequency oscillations assuming a time convention $\exp(-i\omega t)$ are^{4,9,16}

$$-i \omega \rho_0 v_z(x,y,z) = -\frac{dP_1(z)}{dz} + \eta \nabla_\tau^2 v_z(x,y,z), \quad (1)$$

$$-i \omega \rho_1(x,y,z) + \frac{\partial(\rho_0(z) v_z(x,y,z))}{\partial z} + \rho_0(z) \nabla_\tau \cdot v(x,y,z) = 0, \quad (2)$$

$$\rho_1(x,y,z) = -\rho_0(z) \beta T_1(x,y,z) + \frac{\gamma}{c^2} P_1(z), \quad (3)$$

$$-i \omega \rho_0(z) c_p T_1(x,y,z) + \rho_0(z) c_p v_z(x,y,z) T_{0z} = -i \omega \beta T_0 P_1(z) + \kappa \nabla_\tau^2 T_1(x,y,z), \quad (4)$$

where the transverse gradient and Laplacian operators are defined by $\nabla_\tau = \partial/\partial x \hat{x} + \partial/\partial y \hat{y}$ and $\nabla_\tau^2 = (\partial^2/\partial x^2 + \partial^2/\partial y^2)$, and η is gas viscosity. In order, these equations approximately express the z component of the equation of motion, continuity or mass conservation, equations of state for density, and heat transfer. Except for the very important term $T_{0z} = dT_0/dz$ in Eq. (4), these are

the equations given by Zwicker and Kosten¹¹ in their solution for the propagation of sound in circular pores. Equation (4) expresses that the temperature at a fixed position changes due to motion of the ambient fluid, due to compression of the gas, and due to heat conduction. Boundary conditions are $v(x,y,z)=0$ and $T_1(x,y,z)=0$ at the pore boundary.

The time averaged energy flow to second order (subscript 2) is^{9,16}

$$\bar{H}_2(z) = \bar{Q}_2(z) + \bar{W}_2(z) - \bar{Q}_{loss}(z) \quad (5)$$

where time averaged heat flow due to hydrodynamic transport is

$$\bar{Q}_2(z) = \frac{\Omega A_{res}}{2} Re \frac{1}{A} \int (\rho_0 c_p v_z(x,y,z) T_1^*(x,y,z) - \beta T_0 v_z(x,y,z) P_1^*(z)) dx dy ; \quad (6)$$

the heat flow by conduction down a temperature gradient is

$$\bar{Q}_{loss}(z) = \Omega A_{res} \kappa_{gas} T_{0z} + (1 - \Omega) A_{res} \kappa_{stack} T_{0z} ; \quad (7)$$

and the time averaged work flow (or power) is

$$\bar{W}_2(z) = \frac{\Omega A_{res}}{2} Re \frac{1}{A} \int v_z(x,y,z) P_1^*(z) dx dy . \quad (8)$$

Here A_{res} is the cross-sectional area of the resonance tube at point z , A is the cross-sectional area of a single pore, Ω is porosity, κ_{gas} and κ_{stack} are the thermal conductivity of the gas and stack, $*$ indicates complex conjugation, and Re indicates the real part of the expression. The product (ΩA_{res}) is cross-sectional open area of the tube at position z .

Viscous and thermal boundary layer thicknesses are given by $\delta_v = (2\eta/\omega\rho_0)^{1/2}$ and $\delta_\kappa = (2\kappa/\omega\rho_0 c_p)^{1/2}$. We introduce a dimensionless "shear wave number" $\lambda = R(\rho_0\omega/\eta)^{1/2}$ or $\lambda = 2^{1/2} R/\delta_v$, where R is a characteristic transverse dimension of the pore in Fig. 1c, and a dimensionless thermal disturbance number $\lambda_T = R(\rho_0\omega c_p/\kappa)^{1/2}$ or $\lambda_T = 2^{1/2} R/\delta_\kappa$. Use of the Prandtl number $N_{pr} = \eta c_p/\kappa$ gives the relation $\lambda_T = \lambda N_{pr}^{1/2}$. For definiteness, take R to be twice the ratio of the transverse pore area to the pore perimeter so for a circular or square pore, R is the pore radius. Consider the newly named *single pore transport function* $F(x,y,\lambda)$ defined by the following partial differential equation:

$$F(x,y;\lambda) + \frac{R^2}{i\lambda^2} \nabla_{\tau}^2 F(x,y;\lambda) = 1, \quad (9)$$

subject to the boundary condition that $F(x,y,\lambda) = 0$ at the (arbitrary perimeter) pore wall in Fig. 1c. In anticipation of later developments, averages over the pore cross-section, defined for example by $F(\lambda) = A^{-1} \int F(x,y;\lambda) dx dy$ where A is the area of the pore cross-section, are taken. Acoustic particle velocity (1) and temperature (4) are given in terms of pressure and F by the relations

$$v_z(x,y,z) = \frac{F(x,y;\lambda)}{i\omega\rho_0} \frac{dP_1(z)}{dz}, \quad (10)$$

$$T_1(x,y,z) = \frac{\gamma - 1}{c^2 \rho_0 \beta} F(x,y;\lambda_T) P_1(z) - \frac{T_{0z}}{\rho_0 \omega^2} \frac{F(x,y;\lambda_T) - N_{pr} F(x,y;\lambda)}{1 - N_{pr}} \frac{dP_1(z)}{dz} \quad (11)$$

The equation for pressure is

$$\frac{\rho_0}{F(\lambda)} \frac{d}{dz} \left(\frac{F(\lambda)}{\rho_0} \frac{dP_1(z)}{dz} \right) + 2\alpha(\lambda,\lambda_T) \frac{dP_1(z)}{dz} + k(\lambda,\lambda_T)^2 P_1(z) = 0, \quad (12)$$

where

$$\alpha(\lambda, \lambda_T) = \frac{\beta T_{0z}}{2} \left(\frac{F(\lambda_T)/F(\lambda) - 1}{1 - N_{pr}} \right), \quad (13)$$

and

$$k(\lambda, \lambda_T)^2 = \frac{\omega^2}{c^2} \frac{1}{F(\lambda)} (\gamma - (\gamma - 1) F(\lambda_T)). \quad (14)$$

In the absence of a temperature gradient $T_{0z} = 0$ so $\alpha(\lambda, \lambda_T) = 0$. The complex wavenumber in the pore is then given by $\pm k$ which is the usual form found in porous media modeling.¹¹

SPECIFIC ACOUSTIC IMPEDANCE AND PRESSURE TRANSLATION THEOREMS

The *specific acoustic impedance* of an acoustical medium is equal to the ratio of the total acoustic pressure and *total particle velocity*. The *acoustic impedance* is equal to the ratio of the total acoustic pressure and the *total volume velocity*. For porous media the appropriate boundary condition at a surface are continuity of pressure, and continuity of volume velocity or equivalently continuity of acoustic impedance.¹⁶ Volume velocity is $A_{res} V_{zb} = \Omega A_{res} v_z$ where Ω is the porosity, v_z is the actual particle velocity in a pore, and V_{zb} is the average volume velocity per unit area of porous sample. In the analysis of thermoacoustic elements with many pores, v_z is replaced with V_{zb} / Ω in all of the single pore equations. At boundaries between thermoacoustic elements, $P_1(z)$ and $V_{zb}(z)$ or equivalently $Z(z) = P(z) / V_{zb}(z)$ are continuous, where $Z(z)$ is the specific acoustic impedance.

Rayleigh developed an impedance translation theorem for homogeneous fluid layers.¹⁷ The impedance translation theorem relates the specific acoustic impedance at one side of a layer to that at the other. In this manner one may apply the theorem as many times as necessary to compute the specific acoustic impedance at any surface in the layered media. This translation theorem is applicable to heat exchangers and resonator sections, but is not applicable to the stack because the physical parameters such as density, sound speed, etc, depend on z in a continuous manner on

account of the temperature gradient. Impedance and pressure translation theorems which take into account the dependence of physical parameters on position were derived for the stack.¹⁶ The expressions are

$$\frac{dZ(z)}{dz} = i k(z) Z_{int}(z) \left(1 - \frac{Z(z)^2}{Z_{int}(z)^2} \right) + 2 \alpha(z) Z(z), \quad (15)$$

and

$$\frac{dP_1(z)}{dz} = i k(z) Z_{int}(z) \frac{P_1(z)}{Z(z)}, \quad (16)$$

where $\alpha(z)$ and $k(z)$ are given in Eq. (13) and Eq. (14) and

$$Z_{int} = \frac{\rho_0 \omega}{\Omega F(\lambda) k} \quad (17)$$

is analogous to the intrinsic or characteristic impedance of a porous medium. Expressions (15) and (16) are a set of coupled first order differential equations which can be readily solved using numerical techniques. The well-known fourth order Runge-Kutta algorithm is a recommended numerical method. With given values of $P_1(z)$ and $Z(z)$ at position z then pressure and specific acoustic impedance are determined at $z-d$ from use of the algorithm $P_1(z-d) = RK[P_1(z), Z(z)]$ and $Z(z-d) = RK[Z(z)]$ where RK is symbolic notation for the Runge-Kutta algorithm.

For thermoacoustic elements not having temperature gradients (such as heat exchangers and sections of the resonator), Rayleigh's impedance translation theorem¹⁷ can be written for porous media as

$$Z(z-d) = Z_{int} \frac{Z(z) \cos(kd) - i Z_{int} \sin(kd)}{Z_{int} \cos(kd) - i Z(z) \sin(kd)} \quad (18)$$

The pressure translation theorem is

$$P_1(z-d) = P_1(z) \left(\cos(kd) - i \frac{Z_{int}}{Z(z)} \sin(kd) \right) \quad (19)$$

Heat and work flow are

$$\begin{aligned} \bar{Q}_2(z) = & \frac{A_{res}}{2} \frac{\beta T_0}{1 + N_{pr}} \frac{|P_1(z)|^2}{|Z(z)|^2} \left[\operatorname{Re} (Z(z)^* \{ F^*(\lambda_T)/F(\lambda) + N_{pr} \}) \right. \\ & \left. - \frac{T_{0z}}{\beta T_0} \frac{\rho_0 c_p}{\Omega \omega} \frac{1}{|F(\lambda)|^2} \frac{\operatorname{Im} (F^*(\lambda_T) + N_{pr} F(\lambda))}{1 - N_{pr}} \right] - \beta T_0 \bar{W}_2(z), \quad (20) \end{aligned}$$

and

$$\bar{W}_2(z) = \frac{A_{res}}{2} \frac{|P_1(z)|^2}{|Z(z)|^2} \operatorname{Re} Z(z) \quad (21)$$

HEAT AND WORK FLOW IN THE SHORT STACK APPROXIMATION FOR VARIOUS STACK GEOMETRIES

The short stack approximation was devised by Swift⁴ to get an interpretable analytical expression for energy flow using boundary layer theory. For arbitrary pore shapes, see Ref. 16. Figure 1a shows the arrangement for the short stack approximation. Heat exchangers are taken to be of negligible thickness and thus not to affect near-standing wave phasing. The TAE (or stack) of length d is assumed to be short enough that the empty tube standing wave is marginally affected. The temperature difference between opposite ends of the TAE is assumed to be much less than the average temperature at the TAE center so that the thermophysical quantities are approximately constant and are evaluated at the average temperature. TAE porosity is Ω .

With a rigid termination at $z=0$ in Fig. 1a, specific acoustic impedance, pressure, particle velocity amplitude, particle velocity, and particle displacement amplitude and particle displacement at z are, from Eq. (18) and Eq. (19),

$$Z(z) = -i \rho_0 c \cot k_0 z ; \quad (22)$$

and

$$\begin{aligned} P_1(z) &= P_1(0) \cos k_0 z , \quad v_z^s(z) = \frac{P_1(0)}{\Omega \rho_0 c} \sin k_0 z , \quad v_z(z) = i v_z^s(z) , \\ \xi_z^s(z) &= \frac{v_z^s(z)}{\omega} , \quad \xi_z(z) = -\xi_z^s(z) \end{aligned} \quad (23a,b,c,d,e)$$

where the wavenumber in the empty tube is k_0 , the π phase between pressure and particle displacement is due only to the choice of the coordinate system in Fig. 1a, and the actual pore particle velocity and displacement are shown. When z is less than one quarter of a wavelength, $P_1(z)$, $v_z^s(z)$, and $\xi_z^s(z)$ are all greater than zero. Use of (22) and (23) in Eq. (20) gives the heat flow at the hot end of the stack,

$$\begin{aligned} \bar{Q}_2(z) &= -\frac{\Omega A_{\text{res}} P_1(z) v_z^s(z)}{2} \beta T_0 \frac{\text{Im} [F^*(\lambda_T)/F(\lambda)]}{1 + N_{\text{pr}}} \\ &+ \frac{\rho_0 c_p \Omega A_{\text{res}} v_z^s(z)}{2} \frac{\text{Im} \{F^*(\lambda_T) + N_{\text{pr}} F(\lambda)\}}{(1 - N_{\text{pr}}^2) |F(\lambda)|^2} \xi_z^s(z) \frac{T_H - T_C}{d} . \end{aligned} \quad (24)$$

The first term is due to conversion of acoustic power to heat and this heat flows (in the TAE) towards the nearest pressure antinode. The second term is heat transported on account of the temperature gradient and this heat flows in the direction opposite to the positive temperature gradient irregardless of the position of the stack in the standing wave. The terms preceding the

temperature gradient are kind of a dynamical coefficient of thermal conduction. The TAE acts as a refrigerator when the first term is larger than the second. Denote by $T_{0z} = (T_C - T_H)/d$ the temperature gradient across the stack, and denote by Γ the dimensionless critical temperature gradient ratio given by^{9,16}

$$\Gamma = -\frac{T_{0z}}{T_0} \frac{\beta T_0 c \tan(k_0 z)}{\omega \Omega (\gamma - 1)} = -T_{0z} \frac{c_p \tan(k_0 z)}{\omega \Omega \beta T_0 c} \quad (25)$$

In the inviscid approximation for which $N_{pr} = 0$ and $F(\lambda) = 1$,

$$\bar{Q}_2(z) = -\frac{A_{res}}{2} \frac{P_1(0)^2}{\rho_0 c} \beta T_0 \frac{\sin(2k_0 z)}{2} \text{Im} F^*(\lambda_T) (1 - \Gamma) \quad (26)$$

Physically, the term $\text{Im} F^*(\lambda_T)$ is a measure of the dynamical thermal interaction between the gas and solid. If $\Gamma < 1$ heat is transported from cold to hot for $2k_0 z < \pi$. According to Eq. (26), stacks made of pores for which $\text{Im} F^*(\lambda_T)$ is a large value will result in the greatest heat flow.

Work flow is given generally by Eq. (21). No work is done in the region to the left of the stack in Fig. 1a because in this region, pressure and velocity have standing wave phasing. To compute the work done in the stack, use is made of the impedance translation theorem to get the impedance at the right side of the stack.¹⁶ Denote by $V_G = A_{res} \Omega d$ the ambient volume of gas in the TAE. After some manipulation, work flow to first order in $k_0 d$ is

$$\begin{aligned} \bar{W}_2(z) = & -\omega \frac{V_G P_1^2(z)}{2 \rho_0 c^2} (\gamma - 1) \text{Im} F^*(\lambda_T) - \omega \frac{\rho_0 V_G v_z^2(z)}{2} \frac{\text{Im} F^*(\lambda)}{|F(\lambda)|^2} \\ & + \frac{\Omega A_{res}}{2} P_1(z) v_z^2(z) \beta (T_H - T_C) \frac{\text{Im}\{F^*(\lambda_T)/F(\lambda)\}}{1 - N_{pr}} \end{aligned} \quad (27)$$

The first and second terms, always < 0 , are dissipation of potential and kinetic energy per unit time due to thermal and viscous diffusion processes. The third term, which is > 0 when the hot end faces a pressure antinode, is the acoustic power produced on account of the temperature gradient. When the third term is larger than sum of the first two, the TAE produces net acoustic power. Work flow in the inviscid approximation is

$$\bar{W}_2(z) = -\frac{A_{res} \Omega}{2} P_1(0)^2 \frac{T_0 \beta^2 \omega d}{\rho_0 c_p} \text{Im } F^*(\lambda_T) \cos^2(k_0 z) (1 - \Gamma) \quad (28)$$

TAEs made of pores for which $\text{Im } F^*(\lambda_T)$ is a large value will result in the greatest work flow.

Work and heat flow are to be compared for the various pore geometries shown in Fig. 2a-2d. In the inviscid short stack approximation, pores with a large value of $\text{Im } F(\lambda)^*$ will have the greatest heat and work flows as indicated by Eq. (26) and Eq. (28). According to Fig. 5, which shows the real and imaginary parts of $F(\lambda)$ for the various pore geometries, the parallel plate geometry has the largest value of $\text{Im } F(\lambda)^*$. The value occurs for $\lambda_c = 3.2$ which allows one to compute the optimal operating frequency from the relation $\lambda_c = (\rho_0 \omega c_p / \kappa)^{1/2} R$. In other words, you can get about 10% more heat flow and work flow in thermoacoustics by choosing to make your stack from parallel plates rather than the other pore geometries. The functional form of $F(\lambda)$ for the various pore geometries is given in Ref. 16.

DEMONSTRATION AIR-FILLED THERMOACOUSTIC PRIME MOVER

The air-filled thermoacoustic source demonstrated during the lecture is shown schematically in Fig. 6. Heat exchangers were parallel plates of copper and the TAE is a monolithic catalyst support extruded ceramic.¹³⁻¹⁵ The two-microphone-technique impedance-tube¹⁸ at the bottom was removed for the demonstration. The nominally quarter-wavelength resonator was capped at the top with a rigid plate and was open at the bottom. Heat tape was wrapped around the hot end

(the region including the tube at top and the first heat exchanger) followed by heat insulation. Water was circulated around a jacket surrounding the cold heat exchanger. In this way, a temperature gradient was established across the TAE. For sufficiently high temperature gradients, ($\Delta T = 176$ K) the tube produces sound at 116 Hz. The ambient temperature $T_C = 295$ K. The location $z=0$ is nominally a pressure node and particle velocity antinode so the specific acoustic impedance (equal to pressure divided by particle velocity and abbreviated by SAI) is a relative minima for frequencies in the vicinity of the quarter wavelength resonance. All parts were made of copper except the TAE.

SAI measurements were made as a function of the temperature gradient across the stack. The real part is shown in Fig. 7 and imaginary in Fig. 8. Among other uses, these measurements are helpful for evaluating the possibility of using the prime mover as a sound source.¹⁹ One interpretation of Fig. 7 is, for example, that the plane wave reflection coefficient at 80 Hz and $\Delta T = 160$ K is > 1 for waves incident in a tube of the same diameter as the prime mover but in the location of the impedance tube in Fig. 6.²⁰ Also shown as dashed lines in Fig. 7 and 8 is the expression for radiation impedance for a unflanged tube.²¹ The expression is $Z_{rad}(\omega) = -\rho_0 c [(k_0 R/2)^2 - i 0.6 k_0 R]$ where $k_0 = \omega/c$. To determine the frequency of oscillation, we solve for the value of ω such that the complex equation $Z_{rad}(\omega) = Z(\omega)$ measured at $z=0$. The operating point $\Delta T = 176$ K and $f_{res} = 116$ Hz of the prime mover demonstrated is shown by the plus symbol in Figs. 7 and 8.

To validate the theoretical model, SAI, denoted by $Z(z=0; \omega_c)$ can be calculated at $z=0$ using (15) and (18). Most generally, for arbitrary termination impedance $Z_{end}(\omega_c)$ at $z=0$, the frequency of operation is determined by setting $Z_{end}(\omega_c) = Z(z=0; \omega_c)$.²² Here $\omega_c = 2\pi f_{res} - i \pi f_{res}/Q$ is the complex eigenfrequency of the system where f_{res} is the resonant frequency and Q is the quality factor. Notice that ω_c is a function of the tube geometry and of ΔT . The condition $Q \rightarrow \infty$ determines ΔT for onset of acoustic oscillation. The complex eigenfrequency has recently been investigated for a helium or argon-filled prime mover where the resonance tube was sealed at $z=0$ by a rigid cap.²³ A word of caution: For prime movers above onset, or for strongly driven

thermoacoustic refrigerators, the temperature distribution from hot to cold is not determined by (7) alone^{9,16}, and use caution when applying (7) to determine the temperature distribution for a non-driven tube since thermal conductivities depend on temperature. The presence of the strong acoustic wave influences its thermal surroundings⁸ by heat transport and in this sense the thermoacoustic oscillation is an example of a self-interacting wave process.

With the impedance tube removed in Fig. 6, measurements were made of the sound spectrum produced by the prime mover. Figure 9 shows the spectrum for the onset temperature $\Delta T = 176$ K (the peak at 425 Hz was not produced by the prime mover) and for $\Delta T = 209$ K. The ambient temperature was 298 K. A Bruel and Kjaer type 4147 1/2" microphone was placed at $z=0$ in Fig. 6 for these measurements. The electrical power delivered to the heat tape was 220 watts. The value $\Delta T = 209$ K was the steady state equilibrium temperature gradient of the system where heat supplied by the tape was balanced by the sum of the acoustic energy radiated away and dissipated in the resonator, and the heat deposited at the cold heat exchanger due to thermoacoustic transport plus normal heat conduction down the gradient. The acoustic power radiated at 116 Hz and $\Delta T = 209$ K was estimated to be 0.25 watts. Some of the applied heat energy goes into the acoustical energy in the band near 116 Hz, in the higher harmonics, and into the steady DC circulation of gas due to acoustic streaming^{5,24} that occurs out of the prime mover at the center and returns along the walls.²⁵ Evidence of acoustic streaming is indicated in Fig. 9 where the generally elevated background level is due to flow induced noise. A flow velocity of 4 m/s was measured for the gas exiting the central part of the prime mover. It is noteworthy that the eigenfrequencies of the quarter wavelength oscillator are given by $f_{res}(2m+1)$ where $m=0,1,\dots$ and the harmonics of the fundamental due to nonlinear processes⁵ are given by $f_h = f_{res} n$ where $n = 2,3,\dots$. For example, the peak at 232 Hz does not correspond to any eigenfrequency of the tube, but is predicted by the analysis of strong waves in open tubes.⁵ Nonlinearities in closed thermoacoustic oscillators have also been studied.²⁶

Figure 10 shows $\Delta T = 209$ K sound produced by the prime mover with the microphone in the opening and 5.7 cm from the bottom (inside of the tube). At the inside point the sound

pressure level is 145 dB, 116 Hz. The opening corresponds nominally to a pressure node, so the acoustic pressure $\approx \cos(\pi x/2L)$ where x is the distance from the top and $L = 72.7$ cm is the overall length of the prime mover. Consequently the pressure at the top is approximately 8 times the level at 5.7 cm inside, or ≈ 163 dB at 116 Hz. The tube radius $R = 4.32$ cm is much less than the acoustic wavelength $= 297$ cm at 116 Hz, so the prime mover mouth behaves as a point source of spherically expanding waves. Figure 11 shows the sound pressure level for the fundamental at 116 Hz and its harmonics 5.7 cm inside the prime mover, at the mouth, and at distances away from the mouth. Efforts to increase the radiation efficiency of the prime mover in a given direction would result in more radiated acoustic energy and would need to be accommodated by increasing the temperature gradient.

In one experiment the sound production by the prime mover was suppressed and it was super-heated to $\Delta T = 285$ K, well beyond the minimal onset $\Delta T = 176$ K. Figure 12 shows the time evolution of the super-heated prime mover. A microphone was placed ≈ 14 cm from the mouth for this measurement. The top figure shows the first 0.6 seconds. Up to 1.4 seconds the amplitude grows exponentially with time and beyond it begins to level off. The bottom figure is a peak detection of the maximal pressure amplitude, the beginnings of which is shown in the top figure. Between 1.5 and 2 seconds the prime mover flutters as shown on the bottom figure and is apparent to an observer. During this time the built-up heat in the hot end is used up by sound production and thermoacoustic heat transport down the temperature gradient. After 2 seconds the prime mover makes a long transition to a steady-state pressure level and the temperature at the hot end slowly diminishes to the steady state equilibrium value $\Delta T = 209$ K. The time evolution of a non superheated prime mover has been studied by Muller, et. al.²⁷

NUMERICAL RESULTS FOR A HELIUM-FILLED PRIME MOVER

Figure 13 is a summary of the UM thermoacoustic engine. Design criteria for this tube was that it would produce sound at as small a temperature gradient as possible given the constraints on construction of parts. After construction the TAE was put through tests to see if onset would occur

and indeed it did. The tube was filled mostly with Helium to a pressure of 3 kPa. Appendix A contains the programs used for the results discussed in this section.

Figure 14 shows the computed stability curve for the fundamental frequency near 308 Hz and the 1st harmonic near 605 Hz. Ambient pressure is the horizontal axis. Temperature difference between hot and cold ends is on the vertical axis. For temperatures below the boundary between stable and unstable no gas oscillations occur. Thermal boundary layer thickness $\delta_T = (2\kappa/\rho_0\omega c_p)^{1/2} \propto \omega^{-1/2} P_0^{-1/2}$ where P_0 is the ambient pressure in the tube. For fixed tube length as in the UM TAE, the boundary layer thickness can be adjusted by changing P_0 . For low P_0 , the boundary layer is much thicker than the pore size in the stack and heat exchangers so gas viscosity chokes the flow. For $P_0 = 173$ kPa the boundary layer thickness is optimal for thermoacoustic effects and the lowest onset temperature of around 180 C occurs. One factor that greatly contributes to minimizing the onset temperature is the location of the stack and heat exchangers relative to the lengths of the hot and cold ends. When the elements are too close to the hot end gas particle displacement is small so the required temperature gradient as computed from τ (25) becomes prohibitively large. When you try to do work on the gas it responds by changing pressure but only a small particle displacement occurs. However as the elements move too close to the center of the tube where a pressure node occurs the work done approaches zero. When you try to do work on the gas at this point in the standing wave the gas responds by undergoing a large displacement, but only a small pressure change occurs. Somewhere between the pressure node at the center and the particle velocity node at the end is an optimal location for the location of the elements. The optimal location is closer to the end where particle velocity is less so that losses due to gas viscosity are minimal. The UM TAE was designed to optimize the location of the elements.

Since $\delta_T \propto T_0^{0.8} \omega^{-1/2} P_0^{-1/2}$ it seems odd at first glance that the minimum of the first harmonic would be at a higher pressure than the fundamental. The temperature dependence is in part due to ambient density and in part to thermal conductivity. Supposing there to exist an optimal boundary layer thickness, then as ω is increased, P_0 should decrease to balance the equation. However, there is no single optimal boundary layer thickness for the tube. Viscous losses can be

defeated by aiming at thin boundary layers. The stack location in the UM TAE helps to minimize viscous losses for the fundamental, but not the first harmonic. Additionally, particle displacement is smaller at higher frequencies so the necessary temperature gradient $|T_{Oz}|$ in Eq. (25) to make $\Gamma > 1$ for onset increases. (The pressure in the standing wave changes from maximum to minimum over a shorter distance as the frequency increases.) At a frequency double the fundamental, the ambient pressure must diminish by a factor of $2^{1/2}$ to get the same optimal boundary layer thickness. But according to Eq. (25) the average temperature $(T_H + T_C)/2$ must increase by a factor of 2. To offset the temperature increase, the ambient pressure must increase by a factor of $2^{0.8}$. Thus it is reasonable that the ambient pressure must increase by a net amount approximately equal to $2^{0.3}$ to achieve the boundary layer thickness for optimal thermoacoustic pumping of the wave. In order to experimentally observe both modes, the TAE should be heated to a temperature in the unstable region of the 1st harmonic with the Q of the resonant cavity so low that there is no oscillation of the fundamental. When the Q is increased, both modes should oscillate.

Figure 15a is the $1/Q$ curve for the fundamental and 1st harmonic for a pressure of 173 kPa. When $1/Q = 0$ the TAE is at the perilous boundary between stability and instability. For ΔT above the onset value 154.6 K for the fundamental, the time evolution of the pressure follows the form $\exp(\pi f_0 t / |Q|)$ until nonlinearity becomes apparent.²⁷ The exponential growth factor for the fundamental has a maximum at $\Delta T = 800$ K. For higher temperatures the ambient temperature in the hot end causes the ambient sound speed, which is $c \propto T_0^{1/2}$, to increase. As a rough guide for computing the resonant frequency of the tube, note that resonance should occur for $2k_{0c}L_c + 2k_{0h}L_h = 2\pi$ or alternatively $f_0 = 1/[2(L_c/c_c + L_h/c_h)]$ where L_c and c_c are the lengths and sound speeds of the cold section, etc. Thus as c_h increases we can view this as an effective shortening of the hot end, which puts the elements closer to a velocity node with concomitant decrease of effectiveness. We can also understand the increase of the resonant frequency with temperature shown in Fig. 15b from the equation for f_0 . Dispersion effects in the thermoacoustic elements are somewhat apparent in this figure in that the frequency of the first harmonic is not twice the

fundamental. This difference is much more noticeable in the original numbers from which these files were made.

GENERAL PRIME MOVER ANALYSIS USING ENERGY BOUNDARY CONDITIONS

We have analyzed prime movers by assuming the temperature distribution in the stack from hot to cold was simply of the form $T_0(z) = T_{0cold} + z(T_{0hot} - T_{0cold})/d$ where d is stack length. This assumption is generally invalid for two reasons. First, even for temperature gradients below onset, temperature dependence of the thermal conductivities of the stack and gas cause the ambient temperature distribution to differ from the simple form above. This is seen in Ref. 8. Treating the heat flow like a electrical current, the applied temperature difference at both ends as voltage, and the stack and gas as resistors, net resistance is the parallel combination of gas and stack. The gas and stack can each individually be considered series combinations of resistors with each resistor being a locally isothermal section of the stack or gas. Just as most of the voltage is dropped across the largest resistor in a series circuit, the largest temperature gradient occurs in the stack where the thermal conductivity is lowest. For gases and many materials, thermal conductivity increases with temperature so the largest temperature gradients will be near the cold end of the stack. The second reason that the assumed simple form for the temperature distribution is invalid occurs for the prime mover above onset. The heat flow equation (20) has a term proportional to temperature gradient and dependent on the product of pressure and particle velocity. This term is a dynamic coefficient of thermal conductivity that depends on position and the square of the pressure amplitude.

For a given heat supply the prime mover can reach a steady equilibrium state. Heat supplied at the hot end is converted into acoustic energy and also transported down the temperature gradient to the cold end. No heat is transferred from the stack to an external source or sink. Consequently the energy flow on the left hand side of Eq. (5) H_2 is a constant in the stack. Merkli and Thomann, Ref. 6, showed that $\partial H_2 / \partial z$ is proportional to the amount of heat transferring to the wall at location z , and the net heat transferring to the wall is naturally the integral over the same the wall length in question. Swift^{8,9} uses the fact of H_2 constant to determine numerically the steady state

equilibrium of the prime mover. The prime mover can be analyzed from a steady state perspective as follows. Given boundary or initial conditions are: heat supplied at the hot exchanger, the cold end temperature, and the ambient pressure in the tube. Determine: The acoustic pressure, temperature at the hot end, and the frequency of operation. Solution: Assume an acoustic pressure at the rigid end of the prime mover. Assume a hot end temperature and frequency of operation. Use impedance translation to get the pressure and impedance at the hot heat exchanger, stack interface. Compute H_2 = heat supplied at the hot exchanger plus H_2 computed from use of equation (5). Since H_2 is a constant in the stack, the value computed at the hot heat exchanger, stack interface is the same throughout the stack. Solve Eq. (5) for the temperature gradient and numerically integrate impedance, pressure, and temperature through the stack to the cold end. Here you must end up with the temperature being equal to the cold end temperature: if not, then some of the assumed quantities are wrong. Assuming that the loop has determined the correct pressure and hot end temperature, the specific acoustic impedance looking into the cold heat exchanger must be equal to the SAI looking down the tube towards the termination at the cold end. If not, then the frequency of operation must be adjusted and the code should start the whole loop over. That impedance looking each way is the same simply occurs due to conservation of pressure and volume velocity in the tube. An alternative approach, or at least a mechanism to use to check for energy conservation, which has some merit is energy conservation. The heat entering the system must be equal to the sum of heat leaving at the cold end plus acoustic energy by the first law of thermodynamics.

SUNDERY REMARKS

A series of interesting fundamental investigations have been performed using a single circular tube for which the thermal boundary layer thickness was approximately equal to the tube radius.²⁸⁻
³¹ Their basic arrangement was a tube closed at one end by a pressure transducer and at the other by varying transducers depending on the particular situation under study. The gaseous helium filled tube was bent to a U-shape and the U-portion was immersed in cold helium gas at

temperatures in the range 4.2 to 45 K.²⁹ The hot end was held at room temperature. They investigated the stability curve of the second tube mode,³¹ the stability curve of the fundamental mode under a variety of conditions,³⁰ the universal properties of a thermoacoustic oscillator at the intersection of the stability curve of the first and second modes,²⁹ and the universal properties of a driven thermoacoustic oscillator.²⁸ On the practical side, thermoacoustics refrigeration has been a recent topic of investigation.³²⁻³⁵ Traveling wave thermoacoustic engines utilizing the Stirling thermodynamic cycle have also been of recent interest.^{36,37}

Future work might include the following. Numerically simulate the Lagrangian picture of thermoacoustics including viscosity and temperature gradients and a variety of capillary tube shapes. This would enhance the intuitive understanding of thermoacoustics and would possibly lead to new designs for thermoacoustic elements. Construct and analyze a prime mover where the tubes have increasing radii from the cold to hot end so that the optimal thermal boundary layer thickness (which is temperature dependent) is achieved at all positions. Theory indicates variable tube radii should lead to more efficient operation.^{34,38} A major effort could be expended in both theoretically and experimentally determining the role of acoustic streaming⁵ in thermoacoustics. The present theory²⁴ of thermoacoustic streaming is only a boundary layer theory. Someone should build and investigate more thoroughly the radial-wave thermoacoustic engine.⁹ A comprehensive design program could and should be written for thermoacoustic engines, given the present state of theoretical development. Stability curves like the type described in Refs 28-31 could be determined for arrangements more typical of practical devices such as that shown in Fig. 1. We have recently completed construction of a minimal ΔT_{onset} closed helium prime mover system which is fully instrumented and will be analyzed in the near future. Much of the numerical work for this system has already been done.

Swift has recently supplied me with a draft of a paper on the performance of a large thermoacoustic prime mover.³⁹ In it he establishes a first crack at the mature stage of thermoacoustics. Though we all know nonlinearity is a general frontier at the moment, Swift and to some extent Muller²⁵ were first to establish calculation techniques in thermoacoustics. As Ralph

Goodman once said, and I paraphrase, linear acoustics is women's work. He was paraphrasing an Englishman himself. However, after viewing the work of women at the Univ. of Texas on nonlinear acoustics, I think his statement should have "women's" replaced with "wimp's". One obvious feature of prime movers is that the large acoustic amplitudes result in harmonic production. Swift treated the 1st harmonic as being due to a source at the end and included the thermoacoustic effects in a calculation. I see no reason, other than wimpdom, to quit at the first harmonic. One must first learn how to compute the amount of harmonic produced for a given fundamental. Then with a steady state relation between harmonics and the fundamental, the overall system can be treated much in the same manner as approached by Swift. He neglected the effects of the acoustic wind (or streaming) in his calculation, but some accounting of the energy consumed by it should be possible. Though my statements here are very sketchy, Swift's work³⁹ indicates this is an approachable frontier area of thermoacoustics. He finds satisfactory agreement in almost all cases when linear thermoacoustics is valid. It is necessary to understand the nonlinear problem if one wants to design practical high power thermoacoustic engines.

REFERENCES

1. J. W. Strutt Lord Rayleigh, *Theory of Sound* (two volumes), (New York, Dover, 1945 re-issue) Vol. II Secs. 322f and 322g.
2. K. W. Taconis, J. J. M. Beenakker, A. O. C. Nier, and L. T. Aldrich, "Measurements concerning the vapour-liquid equilibrium of solutions of He^3 and He^4 below 2.19 K", *Physica* 15, 733-739 (1949).
3. N. Rott, "Damped and thermally driven acoustic oscillations in wide and narrow tubes," *Z. Angew. Math. Phys.* 20 230-243 (1969).
4. N. Rott, "Thermoacoustics," *Adv. Appl. Mech.* 20, 135-175 (1980).
5. O. V. Rudenko, S. I. Soluyan, *Theoretical Foundations on nonlinear acoustics*, (Plenum, New York, 1977).
6. P. Merkli and H. Thomann, "Thermoacoustic effects in a resonance tube," *J. Fluid Mech.* 70, 161-177 (1975).
7. J. Wheatley, T. Hofler, G. W. Swift, and A. Migliori, "Experiments with an intrinsically irreversible acoustic heat engine," *Phys. Rev. Lett.* 50, 499-502 (1983).

8. J. Wheatley, T. Hofler, G. W. Swift, and A. Migliori, "An intrinsically irreversible thermoacoustic heat engine," *J. Acoust. Soc. Am.* **74**, 153-170 (1983).
9. G. W. Swift, "Thermoacoustic engines," *J. Acoust. Soc. Am.* **84**, 1145-1180 (1988).
10. N. Rott, "Thermoacoustic heating at the closed end of an oscillating gas column," *J. Fluid. Mech.* **145**, 1-9, (1984). See pg. 5 in particular.
11. C. Zwikker and C. Kosten, *Sound Absorbing Materials* (Elsevier, Amsterdam, 1949).
12. M. R. Stinson, "The propagation of plane sound waves in narrow and wide circular tubes, and generalization to uniform tubes of arbitrary cross-sectional shape," *J. Acoust. Soc. Am.* **89**, 550-558, (1991).
13. The ceramics are manufactured by, among others, Corning Incorporated, Industrial Products Division, Corning, New York, 14831. For a discussion of their properties, see J. J. Burton and R. L. Garten, *Advanced Materials in Catalysis* (Academic Press, New York, 1977) Chapter 10, and I. M. Lachman, "Monolithic Catalyst Systems," *Alumina Chemicals Science and Technology Handbook*, 283-288, (1990).
14. H. S. Roh, W. P. Arnott, J. M. Sabatier, and R. Raspet, "Measurement and calculation of acoustic propagation constants in arrays of small air-filled rectangular tubes," *J. Acoust. Soc. Am.* **89**, 2617-2624, (1991).
15. W. P. Arnott, J. M. Sabatier, R. Raspet, "Sound propagation in capillary-tube-type porous media with small pores in the capillary walls," In press, *J. Acoust. Soc. Am.*
16. W. P. Arnott, H. E. Bass, R. Raspet, "General formulation of thermoacoustics for stacks having arbitrarily-shaped pore cross-sections," In press, *J. Acoust. Soc. Am.*
17. A. D. Pierce, *Acoustics: An Introduction to Its Physical Principles and Applications* (American Institute of Physics, New York, 1989).
18. A. F. Seybert and D. F. Ross, "Experimental determination of acoustic properties using a two-microphone random-excitation technique," *J. Acoust. Soc. Am.* **61**, 1362-1370 (1977).
19. T. B. Gabrielson, "Radiation from a submerged thermoacoustic source," *J. Acoust. Soc. Am.* **90**, 2628-2636 (1991).
20. Reference 17, p. 109.
21. L. E. Kinsler, A. R. Frey, A. B. Coppens, and J. V. Sanders, *Fundamentals of Acoustics* (Wiley, New York, 1982), 3rd ed., p. 202.
22. W. P. Arnott, R. Raspet, H. E. Bass, "Complex eigenfrequency analysis of thermoacoustic heat engines," *J. Acoust. Soc. Am. Suppl.* **1** **89**, S2007 (1991).
23. A. Atchley, H. E. Bass, T. J. Hofler, and H. T. Lin, "Study of a thermoacoustic prime mover below onset of self-oscillation," In press, *J. Acoust. Soc. Am.*
24. N. Rott, "The influence of heat conduction on acoustic streaming," *Z. Angew. Math. Phys.* **25** 417-421 (1974).

25. E. N. Andrade, "On the circulations caused by the vibration of air in a tube," Proc. Roy. Soc. (London) A134, 445-470, (1931).
26. A. A. Atchley, H. E. Bass, and T. J. Hofler, "Development of nonlinear waves in a thermoacoustic prime mover," in *Frontiers of Nonlinear Acoustics: Proceedings of 12th ISNA*, ed. M. F. Hamilton and D. Blackstock (Elsevier, London, 1990) 603-608.
27. V. A. A. Muller, E. Lang, "Experimente mit thermisch getriebenen Gas-Flussigkeits-Schwingungen," Z. Angew. Math. Phys. 36 358-366 (1985).
28. T. Yazaki, S. Sugioka, F. Mizutani, and H. Mamada, "Nonlinear dynamics of a forced thermoacoustic oscillation," Phys. Rev. Lett. 64, 2515-2518 (1990).
29. T. Yazaki, S. Takashima, and F. Mizutani, "Complex quasiperiodic and chaotic states observed in thermally induced oscillations of gas columns," Phys. Rev. Lett. 58, 1108-1111 (1987).
30. T. Yazaki, A. Tominanga, and Y. Narahara, "Experiments on thermally driven acoustic oscillations of gaseous helium," J. Low Temp. Phys. 41, 45-60 (1980).
31. T. Yazaki, A. Tominanga, and Y. Narahara, "Thermally driven acoustic oscillations: Second harmonic," Phys. Lett. 79A, 407-409 (1980).
32. Hofler, T. J., *Thermoacoustic refrigeration design and performance*, Ph.D. Dissertation, Univ. CA, San Diego, CA, 1986. See also Ref. 9.
33. R. B. Byrnes, *Electronics for autonomous measurement and control of a thermoacoustic refrigerator in a space environment*, Masters Thesis, Naval Postgraduate School, Monterey, CA, 1989.
34. G. A. Bennett, *Active cooling for downhole instrumentation: Miniature thermoacoustic refrigerator*, Ph.D. Thesis, Univ. of NM, Albuquerque, NM, 1991.
35. G. W. Swift and R. A. Martin, "First measurements with a thermoacoustic driver for an orifice-pulse-tube refrigerator," J. Acoust. Soc. Am. Suppl. 1 88, S95 (1990).
36. P. H. Ceperley, "Gain and efficiency of a short traveling wave heat engine," J. Acoust. Soc. Am. 77, 1239-1244 (1985).
37. P. H. Ceperley, "A pistonless stirling engine-The traveling wave heat engine," J. Acoust. Soc. Am. 66, 1508-1513 (1979).
38. N. Rott, and G. Zouzoulas, "Thermally driven acoustic oscillations, Part IV: Tubes with variable cross-section," Z. Angew. Math. Phys. 27 197-224 (1976).
39. G. W. Swift, "Analysis and performance of a large thermoacoustic engine", draft received 5 Nov. 1991. He said the paper was submitted also to J. Acoust. Soc. Am.

FIGURE CAPTIONS

- Fig. 1. a) Generic arrangement used in thermoacoustic heat engines. b) An exposed view of a thermoacoustic element consisting of a parallel combination of square capillary tubes. c) A single arbitrary-perimeter capillary tube for use in a thermoacoustic element.

- Fig. 2. a) Parallel plate, b) circular, c) rectangular, and d) equilateral triangular capillary tube geometries.
- Fig. 3. Lagrangian view of a fluid parcel in a standing wave near a boundary.
- Fig. 4. Magnitude and phase of the excess temperature between parallel plates.
- Fig. 5. Real and imaginary part of the $F(\lambda)$ different pore geometries.
- Fig. 6. Demonstration thermoacoustic oscillator and analysis impedance tube.
- Fig. 7. Real part of the specific acoustic impedance at the mouth of the prime mover.
- Fig. 8. Imaginary part of the specific acoustic impedance.
- Fig. 9. Prime mover sound spectrum for onset $\Delta T = 176$ K and a higher $\Delta T = 209$ K.
- Fig. 10. Prime mover sound spectrum for $\Delta T = 209$ K in the mouth and 5.7 cm inside of the prime mover.
- Fig. 11. Spectral peaks as a function of distance from the mouth of the prime mover.
- Fig. 12. Time evolution of the superheated prime mover.
- Fig. 13. Scale drawing of the constructed UM helium filled prime mover.
- Fig. 14. Stability curves for the fundamental and first harmonic for the UM TAE.
- Fig. 15. a) Quality factor and b) resonant frequency for the UM TAE with ambient pressure 173 kPa

PUBLICATIONS

Heui-Seol Roh, W. Patrick Arnott, James M. Sabatier, and Richard Raspet, "Measurement and calculation of acoustic propagation constants in arrays of small air-filled rectangular tubes," *J. Acoust. Soc. Am.* 89, 2617-2624 (1991).

W. Pat Arnott, Henry E. Bass, and Richard Raspet, "General formulation of thermoacoustics for stacks having arbitrarily shaped pore cross sections," *J. Acoust. Soc. Am.* 90, 3228-3237 (1991).

W. Patrick Arnott, James M. Sabatier, and Richard Raspet, "Sound propagation in capillary-tube-type porous media with small pores in the capillary walls," *J. Acoust. Soc. Am.* 90, 3299-3306 (1991).

PRESENTATIONS

W. Pat Arnott, Richard Raspet, and Henry E. Bass, "Complex eigenfrequency analysis of thermoacoustic heat engines," 89 (4), (1991).

**APPENDIX: FORTRAN PROGRAM FOR ANALYSIS OF THE UM TAE
EXECUTION FILE FOR THE THERMOACOUSTIC ENGINE CODE. THE CODE
IS ON MY ACCOUNT ON THE IBM 3084, CMS OPERATING SYSTEM
MACHINE. ACCESS: LOGIN PAARNOTT, PASSWORD FROGGY.**

```
&IF &INDEX NE 0 &GOTO -HEREWEGO
&TYPE ENTER THE NAME OF THE PARAMS FILE WHICH DESCRIBES THE TAE.
&READ ARGS
-HEREWEGO
VMFCL:AR
COPYFILE &1 PARAMS A TEMP PARAMS A (REPLACE
EXEC GLOBALS
FILEDEF 1 DISK T DATA A
FILEDEF 2 DISK TEMP PARAMS A
FILEDEF 15 DISK PRESS DATA A (RECFM V
FILEDEF 16 DISK WORKFLOW DATA A (RECFM V
FILEDEF 17 DISK HEATFLOW DATA A (RECFM V
FILEDEF 18 DISK IMPED3D DATA A (RECFM V
FILEDEF 19 DISK IMPED DATA A (RECFM V
FILEDEF 20 DISK ENTHALPY DATA A (RECFM V
FILEDEF 21 DISK WORKDRIV DATA A (RECFM V
FILEDEF 27 DISK QUALREC DATA A
FILEDEF 28 DISK RESFREQ DATA A
FILEDEF 29 DISK QUALFACT DATA A
FILEDEF 30 DISK POSVSDT DATA A
FILEDEF 37 DISK QUALREC DATAEIG A
FILEDEF 38 DISK RESFREQ DATAEIG A
FILEDEF 39 DISK QUALFACT DATAEIG A
FILEDEF 41 DISK T02 DATA A
FILEDEF 42 DISK REIMPED DATA A (RECFM V
FILEDEF 43 DISK IMIMPED DATA A (RECFM V
FILEDEF 44 DISK STABCURV DATA A (RECFM V
* PROGRAM FOR COMPUTING PROPAGATION CONSTANTS...
*LOAD TAEUTIL ( CLEAR NOMAP START
* GENERAL PROGRAM FOR COMPUTING Z,P,HEAT,WORK.
*LOAD TAEHE2 ( CLEAR NOMAP START
* GENERAL PROGRAM, FINITE DIFF IN STACK, FOR COMPUTING Z,P,HEAT,WORK.
*LOAD TAEHE3 ( CLEAR NOMAP START
* GENERAL PROGRAM, FINITE DIFF IN STACK, FOR COMPUTING Z,P,HEAT,WORK.
* GAS ABSORPTION IS INCLUDED IN THE OPEN TUBE SECTIONS.
*LOAD TAEHE3V2 ( CLEAR NOMAP START
* GENERAL PROGRAM, RUNGE KUTTA IN STACK, FOR COMPUTING Z,P,HEAT,WORK.
*LOAD TAERUNGE ( CLEAR NOMAP START
* GENERAL PROGRAM, RUNGE KUTTA IN STACK, FOR COMPUTING Z,P,HEAT,WORK.
* CAN ALSO COMPUTE TRAVELING WAVES. SOMEWHAT OPTIMIZED.
*LOAD TAEHEUNG ( CLEAR NOMAP START
* GENERAL PROGRAM FOR COMPUTING Z,P,HEAT,WORK. BASED ON DF/DLAMBDA.
*LOAD TAEHE4 ( CLEAR NOMAP START
* PROGRAM FOR COMPUTING THE Q FROM COMPLEX EIGENFREQUENCY.
*LOAD TAEHEQ ( CLEAR NOMAP START
* PROGRAM FOR COMPUTING THE Q FROM COMPLEX EIGENFREQUENCY.
* USES INPUT FROM TAEHE3 AS INPUT TO START THINGS OFF WITH.
*LOAD TAEHEQ2 ( CLEAR NOMAP START
* ALL RUNGE-KUTTA PROGRAMS ABOVE HERE ARE NOT CORRECTED.
* PROGRAM FOR COMPUTING THE Q AS A FUNCTION OF TEMPERATURE IN AN EASY
* WAY. USES RUNGE KUTTA INTEGRATION.
* SECOND PROGRAM IS A COMPLEX NUMBER VERSION TO GET THE COMPLEX EIG FRE.
*LOAD TAEAUTO ( CLEAR NOMAP START
*LOAD TAECAUTO ( CLEAR NOMAP START
* VERSION OF TAECAUTO FOR AIR FILLED TUBES.
*LOAD TAECAIR ( CLEAR NOMAP START
* TO PLOT 1/Q AND RES VERSUS LAMBDA, USING TAECAIR, FOR A PRIMEMOVER.
*LOAD TAECBALT ( CLEAR NOMAP START
* TAECMONT: PROGRAM BASED ON TAECAUTO TO COMPUTE THE Q AND RESFREQ FOR
```

- * THE MONTEREY TUBE. TAKES INTO ACCOUNT THE DEPENDENCE ON TEMPERATURE
- * WHEN COMPUTING THE THERMAL CONDUCTIVITY OF THE STACK.
- * LOAD TAECMONT (CLEAR NOMAP START
- * UMTAE FORTRAN: PROGRAM FOR DESIGN OF THE UMTAE. USED TAECAUTO AS THE
- * STARTING PROGRAM.
- * LOAD UMTAE (CLEAR NOMAP START
- * UMTAECH: CHECK OF UMTAE WITH MONTEREY DATA
- * LOAD UMTAECH (CLEAR NOMAP START
- * PROGRAM FROM TAECBALT FOR COMPUTING THE RESPONSE OF THE DEMO TAE IN AIR
- * LOAD TAEAIRD (CLEAR NOMAP START
- * UMTAEV2 FORTRAN: PROG FOR DESIGN OF THE UMTAE. USED TAECAUTO AS THE
- * STARTING PROGRAM.
- LOAD UMTAEV2 (CLEAR NOMAP START
- ERASE TEMP PARAMS A
- ERASE FILE SCRATCH A
- FILEDEF * CLEAR
- &EXIT

TAE PARAMETER FILE. ACTUAL #S OF THE UMTAE TUBE.

TAE PARAMETER FILE. ACTUAL #S OF THE UMTAE TUBE.

DEFINE THE TUBE FROM RIGHT TO LEFT. AT LEFT ONE USUALLY HAS THE DRIVER.
MINIMUM FREQUENCY, MAXIMUM FREQUENCY, (HZ), AND NUMBER OF FREQ. POINTS.

250.000 400. 300

TERMINATION AT THE RIGHT END OF THE TUBE.

ONE OF RIGID, FREE, OR INFIN. INFIN IS AN INFINITE TUBE.

RIGID

AMBIENT PRESSURE IN THE TUBE AND THE DRIVER PRESSURE AMPLITUDE FOR ALL
FREQUENCIES. PRESSURE IN PASCAL, DRIVER DISPLACEMENT IN METERS.

3.00D5 1.D-8

NUMBER OF SECTIONS IN THE TAE. E.G. AN OPEN SECTION, RGH HEAT EXCH,
STACK, LEFT HEAT EXCH, AND ANOTHER OPEN SECTION WOULD BE 5. INTEGER.

5

***** DEFINITION OF SECTION 1 *****

SECTION TYPE, ONE OF OPENTU, HEXCH, OR STACK.

OPENTU

ELEMENT TYPE. HAS MEANING ONLY FOR HEXCH OR STACK SECTION TYPES.

ONE OF RECT, CYL, OR SLIT, DEFINING THE TYPE OF PORES.

SLIT

NUMBER OF LAYERS THIS SECTION IS BROKEN UP INTO.

1 <= NUMLAY <= 100 PRACTICALLY.

1

LENGTH OF THE SECTION.

METERS.

23.07D-2

TEMPERATURE OF THE RGH END OF THE SECTION. FOR AN ISOTHERMAL SECTION
SUCH AS OPEN TUBE OR HEAT EXCHANGERS, USE TRGH = TLEFT. KELVIN.

293.00000000000000

TEMPERATURE AT THE LEFT END OF THE SECTION.

SEE NOTE ABOVE. KELVIN.

293.

RATIO OF 2 PORE AREA TO PORE PERIMETER (M). FOR: CYL=RADIUS, SLIT=
WIDTH, RECT=2SW A/(1+A) A>1=SIDES ASPECT RATIO, SW=SHORTEST SEMIWIDTH.

4.281D-2

ASPECT RATIO OF THE PORE. VALID FOR RECTANGULAR PORES ONLY.
NECESSARY AS A GENERAL RULE.

1.0D0

POROSITY OF THE SECTION. FOR OPEN TUBE, USE POROSITY = 1.

FOR OTHER TYPES OF SECTIONS, POROSITY <= 1.

1.D0

END OF SECTION 1. *****

***** DEFINITION OF SECTION 2 *****

SECTION TYPE, ONE OF OPENTU, HEXCH, OR STACK.

HEXCH

ELEMENT TYPE. HAS MEANING ONLY FOR HEXCH OR STACK SECTION TYPES.
ONE OF RECT, CYL, OR SLIT, DEFINING THE TYPE OF PORES.

SLIT

NUMBER OF LAYERS THIS SECTION IS BROKEN UP INTO.

$1 \leq \text{NUMLAY} \leq 100$ PRACTICALLY.

1

LENGTH OF THE SECTION.
METERS.

1.814D-2

TEMPERATURE OF THE RGH END OF THE SECTION. FOR AN ISOTHERMAL SECTION
SUCH AS OPEN TUBE OR HEAT EXCHANGERS, USE TRGH = TLEFT. KELVIN.

293.

TEMPERATURE AT THE LEFT END OF THE SECTION.

SEE NOTE ABOVE. KELVIN.

293.

RATIO OF 2 PORE AREA TO PORE PERIMETER (M). FOR: CYL=RADIUS, SLIT=
WIDTH, RECT=2SW A/(1+A) A>1=SIDES ASPECT RATIO, SW=SHORTEST SEMIWIDTH.

1.118D-3

ASPECT RATIO OF THE PORE. VALID FOR RECTANGULAR PORES ONLY.

NECESSARY AS A GENERAL RULE. ASPECT RATIO $\Rightarrow 1$ ALWAYS.

1.0D0

POROSITY OF THE SECTION. FOR OPEN TUBE, USE POROSITY = 1.

FOR OTHER TYPES OF SECTIONS, POROSITY ≤ 1 .

.64D0

END OF SECTION 2

..... DEFINITION OF SECTION 3

SECTION TYPE, ONE OF OPENTU, HEXCH, OR STACK.

STACK

ELEMENT TYPE. HAS MEANING ONLY FOR HEXCH OR STACK SECTION TYPES.
ONE OF RECT, CYL, OR SLIT, DEFINING THE TYPE OF PORES.

RECT

NUMBER OF LAYERS THIS SECTION IS BROKEN UP INTO.

$1 \leq \text{NUMLAY} \leq 100$ PRACTICALLY. (WAS 20 AT ONE TIME)

25

LENGTH OF THE SECTION.
METERS.

5.08D-2

TEMPERATURE OF THE RGH END OF THE SECTION. FOR AN ISOTHERMAL SECTION
SUCH AS OPEN TUBE OR HEAT EXCHANGERS, USE TRGH = TLEFT. KELVIN.

293.

TEMPERATURE AT THE LEFT END OF THE SECTION.

SEE NOTE ABOVE. KELVIN.

293.

RATIO OF 2 PORE AREA TO PORE PERIMETER (M). FOR: CYL=RADIUS, SLIT=
WIDTH, RECT=2SW A/(1+A) A>1=SIDES ASPECT RATIO, SW=SHORTEST SEMIWIDTH.

.77D-3

ASPECT RATIO OF THE PORE. VALID FOR RECTANGULAR PORES ONLY.

NECESSARY AS A GENERAL RULE. ASPECT RATIO $\Rightarrow 1$ ALWAYS.

1.0D0

POROSITY OF THE SECTION. FOR OPEN TUBE, USE POROSITY = 1.

FOR OTHER TYPES OF SECTIONS, POROSITY ≤ 1 .

.69D0

END OF SECTION 3.

..... DEFINITION OF SECTION 4

SECTION TYPE, ONE OF OPENTU, HEXCH, OR STACK.

HEXCH

ELEMENT TYPE. HAS MEANING ONLY FOR HEXCH OR STACK SECTION TYPES.
ONE OF RECT, CYL, OR SLIT, DEFINING THE TYPE OF PORES.

SLIT

NUMBER OF LAYERS THIS SECTION IS BROKEN UP INTO.

1 \Leftarrow NUMLAY \Leftarrow 100 PRACTICALLY.

1

LENGTH OF THE SECTION.

METERS.

1.638D-2

TEMPERATURE OF THE RGH END OF THE SECTION. FOR AN ISOTHERMAL SECTION
SUCH AS OPEN TUBE OR HEAT EXCHANGERS, USE TRGH = TLEFT. KELVIN.

293.

TEMPERATURE AT THE LEFT END OF THE SECTION.

SEE NOTE ABOVE. KELVIN.

293.

RATIO OF 2 PORE AREA TO PORE PERIMETER (M). FOR: CYL=RADIUS, SLIT=
WIDTH, RECT=2SW A/(1+A) A>1=SIDES ASPECT RATIO, SW=SHORTEST SEMIWIDTH.

1.118D-3

ASPECT RATIO OF THE PORE. VALID FOR RECTANGULAR PORES ONLY.

NECESSARY AS A GENERAL RULE. ASPECT RATIO \Rightarrow 1 ALWAYS.

1.0D0

POROSITY OF THE SECTION. FOR OPEN TUBE, USE POROSITY = 1.

FOR OTHER TYPES OF SECTIONS, POROSITY \Leftarrow 1.

.640D0

END OF SECTION 4.

..... DEFINITION OF SECTION 5

SECTION TYPE, ONE OF OPENTU, HEXCH, OR STACK.

OPENTU

ELEMENT TYPE. HAS MEANING ONLY FOR HEXCH OR STACK SECTION TYPES.

ONE OF RECT, CYL, OR SLIT, DEFINING THE TYPE OF PORES.

SLIT

NUMBER OF LAYERS THIS SECTION IS BROKEN UP INTO.

1 \Leftarrow NUMLAY \Leftarrow 100 PRACTICALLY.

1

LENGTH OF THE SECTION.

METERS.

1.29

TEMPERATURE OF THE RGH END OF THE SECTION. FOR AN ISOTHERMAL SECTION
SUCH AS OPEN TUBE OR HEAT EXCHANGERS, USE TRGH = TLEFT. KELVIN.

293.

TEMPERATURE AT THE LEFT END OF THE SECTION.

SEE NOTE ABOVE. KELVIN.

293.

RATIO OF 2 PORE AREA TO PORE PERIMETER (M). FOR: CYL=RADIUS, SLIT=
WIDTH, RECT=2SW A/(1+A) A>1=SIDES ASPECT RATIO, SW=SHORTEST SEMIWIDTH.

4.261D-2

ASPECT RATIO OF THE PORE. VALID FOR RECTANGULAR PORES ONLY.

NECESSARY AS A GENERAL RULE. ASPECT RATIO \Rightarrow 1 ALWAYS.

1.0D0

POROSITY OF THE SECTION. FOR OPEN TUBE, USE POROSITY = 1.

FOR OTHER TYPES OF SECTIONS, POROSITY \Leftarrow 1.

.995D0

END OF SECTION 5.

FORTTRAN CODE FOR THE UM TAE.

The main program is the only part of this program that is specific to the UM TAE.

.....

..*SUBROUTINE SETVAL * GET THE INPUT PARAMETERS FROM AN EXTERNAL FILE**

.....

SUBROUTINE SETVAL

```

* VARIABLES WHICH DEFINE THE TAE
  CHARACTER*70 SECTYP(100),ETYP(100),TERMIN
  INTEGER NUMLAY(100),NUMSEC,NUMFRE
  REAL*8 DELEM(100),TRGH(100),TLEFT(100),RATIO(100)
  *ASPECT(100),POROS(100),
  *THCOND(100),HECAP(100),PAMB,FREMIN,FREMAX,DDRIVE
  INTEGER J
  CHARACTER DUMMY
  COMMON /VARS1/ SECTYP,ETYP,TERMIN
  COMMON /VARS2/ NUMLAY,NUMSEC,NUMFRE
  COMMON /VARS3/ DELEM,TRGH,TLEFT,RATIO,
  * ASPECT,POROS,THCOND,HECAP,PAMB,FREMIN,FREMAX,DDRIVE
1  FORMAT (A1)
2  FORMAT (A70)
  REWIND 2
  READ (2,1) DUMMY
  READ (2,1) DUMMY
  READ (2,1) DUMMY
    READ (2,*) FREMIN,FREMAX,NUMFRE
  READ (2,1) DUMMY
  READ (2,1) DUMMY
    READ (2,2) TERMIN
  CALL NOPAD(TERMIN)
  READ (2,1) DUMMY
  READ (2,1) DUMMY
    READ (2,*) PAMB,DDRIVE
  READ (2,1) DUMMY
  READ (2,1) DUMMY
    READ (2,*) NUMSEC
    DO 10 J=NUMSEC,1,-1
      READ (2,1) DUMMY
      READ (2,1) DUMMY
        READ (2,2) SECTYP(J)
      CALL NOPAD(SECTYP(J))
      READ (2,1) DUMMY
      READ (2,1) DUMMY
        READ (2,2) ETYP(J)
      CALL NOPAD(ETYP(J))
      READ (2,1) DUMMY
      READ (2,1) DUMMY
        READ (2,*) NUMLAY(J)
      READ (2,1) DUMMY
      READ (2,1) DUMMY
        READ (2,*) DELEM(J)
      READ (2,1) DUMMY
      READ (2,1) DUMMY
        READ (2,*) TRGH(J)
      READ (2,1) DUMMY
      READ (2,1) DUMMY
        READ (2,*) TLEFT(J)
      READ (2,1) DUMMY
      READ (2,1) DUMMY
        READ (2,*) RATIO(J)
      READ (2,1) DUMMY
      READ (2,1) DUMMY
        READ (2,*) ASPECT(J)
      READ (2,1) DUMMY
      READ (2,1) DUMMY
        READ (2,*) POROS(J)
      READ (2,1) DUMMY
      THCOND(J)=0.D0
10  HECAP(J)=0.000
  REWIND 2
  RETURN

```

```

END
.....
* SUBROUTINE NOPAD * GETS RID OF BLANKS IN NAMES .....
.....
SUBROUTINE NOPAD(NAME)
CHARACTER*70 OLD,NEW,NAME
CHARACTER*1 Q(70),N(70)
INTEGER LJ
EQUIVALENCE (OLD,Q(1))
EQUIVALENCE (NEW,N(1))
OLD=NAME
NEW=
*
J=0
DO 10 I=1,70
N(I)=
IF (Q(I).NE.' ') THEN
J=J+1
N(J)=Q(I)
END IF
10 CONTINUE
NAME=NEW
RETURN
END
.....
* SUBROUTINE WFLOW * COMPUTE THE WORK FLOW AT Z .....
.....
SUBROUTINE WFLOW(P1,Z,W2)
REAL*8 W2
COMPLEX*16 P1,Z
W2=CDABS(P1)**2 * DIMAG((0.D0,1.D0)/Z) / 2.D0
RETURN
END
.....
* SUBROUTINE QFLOW * COMPUTE THE HEAT FLOW AT Z .....
* I HAVE ASSUMED THE COEFFICIENT OF THERMAL EXPANSION BETA=1/TEMP. **
.....
SUBROUTINE QFLOW(POROS,P1,Z,FLAM,FLAMT,W,DENS,TOZ,KGAS,KSOLID,Q2)
REAL*8 POROS,DENS,TOZ,KGAS,KSOLID,Q2,NPR,CP,GAMMA
COMPLEX*16 P1,Z,FLAM,FLAMT,W
COMMON /PHYCON/ GAMMA,NPR,CP
Q2=POROS*CDABS(P1)*CDABS(P1)/2.D0
Q2=Q2*DIMAG((0.D0,1.D0)*(DCONJG(FLAMT)/FLAM-1.D0)/
* (POROS*Z*(1.D0+NPR)) -
* TOZ * DENS * CP*(FLAM*NPR +DCONJG(FLAMT)) /
* (POROS**2 * W*(CDABS(FLAM*Z))**2*(1.D0+NPR**2))) -
* TOZ*(POROS*KGAS + (1.D0-POROS)*KSOLID)
RETURN
END
.....
* SUBROUTINE DERIVS * COMPUTE THE DERIVATIVES DZ/DZ AND DP/DZ FOR
* THE RUNGE-KUTTA WORK.
.....
SUBROUTINE DERIVS(ZETA,ZINT,ALPRIM,P,Z,DPDZ,DZDZ)
COMPLEX*16 ZETA,ZINT,ALPRIM,P,Z,DPDZ,DZDZ,IFAC,FAC2
I = (0.D0,1.D0)
FAC = Z/ZINT
FAC = (1.D0 - FAC*FAC)
FAC2 = I * ZETA * ZINT
DZDZ = FAC2 * FAC + 2.D0 * ALPRIM * Z
FAC = I * ZETA * (ZINT - Z*Z/ZINT)
DZDZ = FAC + 2.D0 * ALPRIM * Z
DPDZ = FAC2 * P / Z
RETURN

```

```

END
.....
* SUB STAKPM * GET THE MANY PARAMETERS WHICH ARE TEMPERATURE DEPENDENT
* IN THE STAK. USED FOR RUNGE KUTTA INTEGRATION.
* THE STACK IS ASSUMED TO HAVE POROUS WALLS.
.....
SUBROUTINE STAKPM(ETYPE,W,POROUS,PAMB,T,T0Z,DENS,RATIO,ASPECT,
* FLAM,FLAMT,ZETA,ALPRIM,ZINT)
CHARACTER*70 ETYPE
REAL*8 POROUS,PAMB,T,T0Z,DENS,RATIO,ASPECT
COMPLEX*16 FLAM,FLAMT,ZETA,ALPRIM,ZINT,W,LAMBDA,LAMBDT
* POROUS WALL VARIABLES.
REAL*8 PORTOT,PORWAL,DWALL,WFACT
COMPLEX*16 XI
* SUPPORTING ROLE VARIABLES.
REAL*8 SSPEED,VISC,CP,NPR,GAMMA
COMMON /PHYCON/ GAMMA,NPR,CP
* SET THE POROUS WALL CONSTANTS FOR THE 200 CELL CERAMIC.
* TO TURN OFF THE POROUS WALL CALCULATION JUST LET XI=1.D0 BELOW.
PORWAL = 0.49D0
DWALL = 100.D-6
PORTOT = POROUS*(1.D0 + 2.D0*PORWAL*DWALL/RATIO)
WFACT = GAMMA*(PORTOT-POROUS)/(2.D0*POROUS)
* BEGIN
CALL VDCHE(T,PAMB,VISC,DENS,SSPEED,KGAS)
CALL GETLAM(DENS,VISC,W,RATIO,LAMBDA)
LAMBDT = DSQRT(NPR) * LAMBDA
IF (ETYPE.EQ.'RECT') THEN
CALL FRECT(ASPECT,LAMBDA,FLAM)
CALL FRECT(ASPECT,LAMBDT,FLAMT)
ELSE IF (ETYPE.EQ.'CYL') THEN
CALL FCYL(LAMBDA,FLAM)
CALL FCYL(LAMBDT,FLAMT)
ELSE IF (ETYPE.EQ.'SLIT') THEN
CALL FSLIT(LAMBDA,FLAM)
CALL FSLIT(LAMBDT,FLAMT)
ELSE
STOP
END IF
CALL WNHEX(FLAMT,FLAM,W,SSPEED,ZETA)
ZINT = DENS*W/(POROUS * FLAM * ZETA)
XI = GAMMA - (GAMMA-1.D0)*FLAMT
XI = 1.D0 + WFACT/XI
ZETA = ZETA * XI
ZINT = ZINT/XI
ALPRD = T0Z * (FLAMT/FLAM - 1.D0)/(2.D0 * T * (1.D0 - NPR))
RETURN
END
.....
* SUBROUTINE ZPTRAN * DO THE IMPEDANCE TRANSLATION THEOREM ****
* DO ALSO THE PRESSURE TRANSLATION THEOREM ****
* THIS VERSION IS FOR THE HEAT EXCHANGERS AND OPEN TUBE SECTIONS.
.....
SUBROUTINE ZPTRAN(ZINT,SN,CS,ZZMD,P1,P1MD)
COMPLEX*16 ZZMD,ZINT,SN,CS,CT,P1,P1MD,FAC
CT = CS/SN
FAC = ZINT/Z
ZZMD = ZINT * (CT - (0.D0,1.D0)*FAC)/
* (FAC*CT - (0.D0,1.D0))
P1MD = P1 * (CS - (0.D0,1.D0) * FAC * SN)
RETURN
END
.....
* SUBROUTINE ZRIGID ** IMPEDANCE OF A RIGID TERMINATION.

```

```

.....
SUBROUTINE ZRIGID(DENS,SSPEED,VISC,W,Z)
REAL*8 DENS,SSPEED,VISC,NPR,GAMMA,CP
COMPLEX*16 Z,W,FAC
COMMON /PHYCON/ GAMMA,NPR,CP
FAC = CDSQRT( DENS*SSPEED**2 / (W*VISC) )
Z = (1.D0,1.D0)*DENS*SSPEED*FAC*DSQRT(NPR)/(DSQRT(2.D0)*(GAMMA -
* 1.0D0))
RETURN
END
.....
* SUBROUTINE WNTUBE ** WAVENUMBERS FOR WAVES IN THE OPEN TUBE PARTS.
.....
SUBROUTINE WNTUBE(LAMBDA , W , SSPEED , K)
REAL*8 SSPEED,GAMMA,NPR,LAMBDA,FAC1,CP
COMPLEX*16 K,W
COMMON /PHYCON/ GAMMA,NPR,CP
FAC1 = ( 1.D0 + (GAMMA - 1.D0) / DSQRT(NPR) ) / DSQRT(2.D0)
K = W/SSPEED * ( 1.D0 + (1.D0 , 1.D0) * FAC1 / LAMBDA )
RETURN
END
.....
* SUBROUTINE FTUBE * COMPUTES F(LAMBDA) FOR THE RESONANT TUBE.
.....
SUBROUTINE FTUBE(LAMBDA,FLAM)
COMPLEX*16 LAMBDA,FLAM
FLAM = 1.D0 - (1.D0,1.D0) * DSQRT(2.D0) / LAMBDA
RETURN
END
.....
* SUBROUTINE WNHEX ** WAVENUMBERS FOR WAVES IN THE HEAT EXCHANGERS.
.....
SUBROUTINE WNHEX(FLAMT , FLAM , W , SSPEED , K)
REAL*8 SSPEED,GAMMA,NPR,CP
COMPLEX*16 FLAMT,FLAM,K,W
COMMON /PHYCON/ GAMMA,NPR,CP
K = W/SSPEED * CDSQRT( (GAMMA - (GAMMA - 1.D0)*FLAMT) / FLAM )
RETURN
END
.....
* SUBROUTINE VDCHE ** VISCOSITY, DENSITY, AND SOUND SPEED OF HELIUM
* AS A FUNCTION OF TEMPERATURE AND AMBIENT PRESSURE. ALSO THE THERMAL
* CONDUCTIVITY.
.....
SUBROUTINE VDCHE(TABS , PAMB , VISC , DENS , SSPEED,KGAS)
REAL*8 TABS,PAMB,VISC,DENS,SSPEED,GAMMA,NPR,CP,KGAS
COMMON /PHYCON/ GAMMA,NPR,CP
DENS = PAMB * 4.0D-3 / ( TABS * 8.3143D0 )
* MY EXPRESSION FOR VISCOSITY.
VISC = 1.887D-5 * (TABS / 273.15D0)**0.6567D0
* MY EXPRESSION FOR THERMAL CONDUCTIVITY: NPR = CONSTANT.
KGAS = VISC * CP / NPR
* SWIFT'S EXPRESSION FOR VISCOSITY.
VISC = 5.131D-7 * TABS**0.6441D0
* SWIFT'S EXPRESSION FOR THERMAL CONDUCTIVITY: NPR NOT CONSTANT.
KGAS = 0.0044 * TABS**0.6441D0
* NPR = VISC * CP / KGAS
SSPEED = 972.8D0 * DSQRT(TABS / 273.15D0)
RETURN
END
.....
* SUBROUTINE FSLIT *** COMPUTES F(LAMBDA) FOR PARALLEL SLITS.
.....
SUBROUTINE FSLIT(LAMBDA , FLAM)

```

```

COMPLEX*16 LAMBDA,FLAM,SQRM1,ARGUM,CTANH,AR
SQRM1 = (1.0D0, -1.0D0) / DSQRT( 2.0D0 )
AR = SQRM1 * LAMBDA
ARGUM = CDEXP(-AR)
AR = AR / 2.D0
CTANH = (1.D0 - ARGUM) / (1.D0 + ARGUM)
FLAM = 1.0D0 - CTANH / AR
RETURN
END
.....
* SUBROUTINE FCYL **** COMPUTES F(LAMBDA) FOR CYLINDRICAL PORES.
.....
SUBROUTINE FCYL(LAMBDA, FLAM)
COMPLEX*16 FLAM,SQRI,CBS(2),J0,J1,ARGUM,LAMBDA
INTEGER N
N=2
SQRI = (1.0D0, 1.0D0) / DSQRT( 2.0D0 )
ARGUM = SQRI * LAMBDA
CALL DCBUNS( ARGUM, N, CBS )
J0 = CBS(1)
J1 = CBS(2)
FLAM = 1.0D0 - ( 2.0D0 * J1 ) / ( ARGUM * J0 )
RETURN
END
.....
* SUBROUTINE FRECT **** COMPUTES F(LAMBDA) FOR RECTANGULAR PORES.
* OPTIMIZED BY RANDY ZAGAR, 21 NOVEMBER 1991.
.....
SUBROUTINE FRECT(ASPECT, LAMBDA, FLAM)
REAL*8 PISQ, ASPECT, ASPSQ
REAL*8 XN, XM, FAC, TMN, TNM, TMM
REAL*8 TTERM, SSUM
INTEGER M, N, SUMMAX
COMPLEX*16 SUM, FLAM, YMN, YNM, YMM
COMPLEX*16 FAC1, LAMBDA, TERM
DATA PISQ/9.869604404D0/
DATA FAC/6.57022864D-1/

C FAC1 = PISQ / (LAMBDA * (1.D0 + ASPECT))**2
FAC1R = DREAL(FAC1)
FAC1I = DIMAG(FAC1)

C ASPSQ = ASPECT * ASPECT
SUMMAX = 5
SUM = (0.D0, 0.D0)

C DO 30 M = 1, SUMMAX, 2
XM = DFLOAT(M)
XM = XM * XM

C TMM = XM * (ASPSQ + 1.D0)
YMM = DCMPLX(1.D0 - FAC1I * TMM, FAC1R * TMM)
SUM = SUM + 1.D0 / (YMM * XM * XM)

C DO 40 N = M+2, SUMMAX, 2
XN = DFLOAT(N)
XN = XN * XN

C TMN = (ASPSQ * XM + XN)
YMN = DCMPLX(1.0D0 - FAC1I * TMN, FAC1R * TMN)

C TNM = (ASPSQ * XN + XM)
YNM = DCMPLX(1.0D0 - FAC1I * TNM, FAC1R * TNM)

```

```

TERM = (1.D0/YMN + 1.D0/YT/M) / (XM * XN)
TTERM = TERM * DCONIG(TERM)
SSUM = SUM * DCONIG(SUM)

```

C

- * GUARANTEED ACCURACY FOR THE SUM TO EXPONENT/2. E.G. SUM = SUM + ERROR
- * WHERE 1.D-EXPONENT/2 = ERROR/SUM. COMPARES ON THIS LEVEL OF ACCURACY
- * WITH FRECTO.

```
IF (TTERM .LT. (SSUM*1.0D-10)) GOTO 30
```

C

```

SUM = SUM + TERM
40 CONTINUE
30 CONTINUE
FLAM = SUM * FAC
RETURN
END

```

.....

- * SUBROUTINE FRECTO **** COMPUTES F(LAMBDA) FOR RECTANGULAR PORES.
- * OLD SLOWER VERSION.

.....

```

SUBROUTINE FRECTO(ASPECT, LAMBDA, FLAM)
REAL*8 PLASPECT,ASPSQ
REAL*8 F,XN,XM,FAC
INTEGER M,N,SUMMAX
COMPLEX*16 SUM,FLAM,YMN,LAMBDA,FAC1
* SUMMAX MUST BE AN ODD NUMBER!!!!!!!!!!!!!!
PI = 4.0D0 * DATAN(1.0D0)
FAC1 = PI * PI / ( LAMBDA * ( 1.0D0 + ASPECT ) )**2
FAC = 64.0D0 / PI**4
ASPSQ = ASPECT * ASPECT
SUMMAX = 51
SUM = (0.0D0, 0.0D0)
DO 30 M=SUMMAX,1,-2
XM = DFLOAT(M)
XM = XM*XM
DO 40 N=SUMMAX,1,-2
XN = DFLOAT(N)
XN = XN*XN
YMN = 1.D0 + (0.D0,1.D0) * FAC1 * ( ASPSQ * XM + XN )
40 SUM = SUM + 1.0D0 / ( XM * XN * YMN )
30 CONTINUE
FLAM = SUM * FAC
RETURN
END

```

.....

- * SUBROUTINE QUAFAC COMPUTES THE QUALITY FACTOR AND RESONANT FREQU.

.....

```

SUBROUTINE QUAFAC(AMP,FREQ,Q,RESFRE)
REAL*8 Q,RESFRE,AMP(2000),FREQ(2000),MAXAMP,FREHAF,AMPHAF
REAL*8 AMP2(2000),FREQ2(2000),XC(3),BL(3),BU(3),XSCALE(3)
REAL*8 XGUESS(3),FVALUE,PSCALE(3),RPARAM(7)
INTEGER JJRES,JHALF,NUMDAT,JCOUNT,N,ISTART,IBTYPE,IPARAM(7)
COMMON /QCALC/ AMP2,FREQ2,NUMDAT
EXTERNAL FUNCT1
N = 3
IPARAM(1) = 0
IBTYPE = 0
ISTART = 0
MAXAMP = 0.D0
JCOUNT = 0
DO 10 J=1,2000
IF (AMP(J) .GT. MAXAMP) THEN
MAXAMP = AMP(J)
RESFRE = FREQ(J)
JRES = J

```



```

      END IF
10  CONTINUE
      AMPHAF=MAXAMP/DSQRT(2.D0)
      DO 20 J=1,2000
      IF (AMP(J) .GT. AMPHAF) THEN
      FREHAF = (FREQ(J)+FREQ(J-1))/2.D0
      Q = 0.5D0 * RESFRE / (RESFRE - FREHAF)
      JHALF = J
      GOTO 30
      END IF
20  CONTINUE
30  DO 40 J=JHALF-1,JRES + (JRES-JHALF) + 1
      JCOUNT = JCOUNT + 1
      AMP2(JCOUNT) = AMP(J)
40  FREQ2(JCOUNT) = FREQ(J)
      NUMDAT = JCOUNT
      XGUESS(1) = MAXAMP
      XGUESS(2) = RESFRE
      XGUESS(3) = Q
      DO 50 J=1,3
      XSCALE(J)=1.D0
      FSCALE(J)=1.D0
      BL(J) = XGUESS(J) * .5D0
50  BU(J) = XGUESS(J) * 2.D0
      CALL DRCONF(FUNCT1, N, XGUESS, IBTYPE, BL, BU,
      * XSCALE, FSCALE, IPARAM, RPARAM, XC, FVALUE)
      MAXAMP = XC(1)
      RESFRE = XC(2)
      Q = XC(3)
      RETURN
      END
.....
..... SUBROUTINE FUNCT1 FOR IMSL OPTIMIZATION .....
.....
      SUBROUTINE FUNCT1(N, XC, RMSERR)
      REAL*8 AMP(2000),FREQ(2000),XC(3),RMSERR,MAXSQ,F0,Q,F
      INTEGER NUMDAT,J
      COMMON /QCALC/ AMP,FREQ,NUMDAT
      MAXSQ = XC(1)*XC(1)
      F0 = XC(2)
      Q = XC(3)
      RMSERR = 0.D0
      DO 10 J=1,NUMDAT
      F = FREQ(J)
      RMSERR = ( MAXSQ / (1.D0 + (2.D0*Q*(F-F0)/F0)**2)
      * - AMP(J)*AMP(J))**2 + RMSERR
10  CONTINUE
      RETURN
      END
.....
..... SUBROUTINE GETLAM .....
..... LAMBDA .....
      SUBROUTINE GETLAM(DENS, VISC, W, R, LAMBDA)
      REAL*8 DENS,VISC,R
      COMPLEX*16 LAMBDA,W
      LAMBDA = R * CDSQRT( DENS * W / VISC )
      RETURN
      END
.....
.....
* VERSION 3.0 FOR HELIUM BY PAT ARNOTT, 16 FEB 91 .....
* THIS VERSION USES RUNGE KUTTA SOLUTION FOR THE DE INSIDE OF THE STACK.
* TRANSLATION THEOREMS ARE USED IN OPEN TUBE AND HEAT EXCHANGERS.
* W THE RADIAN FREQUENCY IS ASSUMED COMPLEX EVERYWHERE

```

```

*****
SUBROUTINE TAE(FMIN,FMAX,NFREQ,F0EST)
  COMPLEX*16 W,LAMBDA,LAMBDT,FOFW,FPLUS,SQRI,KA
* GENERIC VARIABLES SUCH AS PHYSICAL PROPERTIES OF THE GAS.
  REAL*8 SSPEED,VISC,CP,NPR,GAMMA,KGAS,KSOLID,ARES
* 2 DEPENDENT ARRAYS....
  PARAMETER (N=5000)
  REAL*8 DENS(N),TAVE(N),T0Z(N),POROUS(N),DSUB(N),ZCOOR(N),Q2(N),
    * W2(N)
  COMPLEX*16 ALPHA(N),K(N),COMDEN(N),FLAM(N),FLAMT(N),Z(N),P1(N)
  LOGICAL INSTAK(N)
* VARIABLES WHICH DEFINE THE TAE
  CHARACTER*70 SECTYP(100),ETYP(100),TERMIN
  INTEGER NUMLAY(100),NUMSEC,NUMFRE,PLOTN
  REAL*8 DELEM(100),TRGH(100),TLEFT(100),RATIO(100),FRENEW
    * ASPECT(100),POROS(100),
    * THCOND(100),HECAP(100),PAMB,FREMIN,FREMAX,DDRIVE,PAMBTM
* DEFINE SOME GLOBAL VARIABLES.
  REAL*8 PI,TWOPI,FMIN,FMAX
  INTEGER NFREQ
* EXTRA VARIABLES NECESSARY FOR RUNGE KUTTA EVALUATION OF THE PROBLEM.
  COMPLEX*16 K1,K2,K3,K4,M1,M2,M3,M4,DPDZ,DZDZ,TFUN
  COMPLEX*16 ZETA,ALPRIM,ZINT,AR,SN,CS
  REAL*8 TNS,TNSM1,F0EST,LEQUTV,RGAS,LSUM,OPL
  INTEGER I,J,JUP,JLOW,NUMTOT,NS
  COMMON /PHYCON/ GAMMA,NPR,CP
  COMMON /VARS1/ SECTYP,ETYP,TERMIN
  COMMON /VARS2/ NUMLAY,NUMSEC,NUMFRE
  COMMON /VARS3/ DELEM,TRGH,TLEFT,RATIO,
    * ASPECT,POROS,THCOND,HECAP,PAMB,FREMIN,FREMAX,DDRIVE
  COMMON /OUTPUT/ P1,Z,Q2,W2,ZCOOR,INSTAK
* ESTABLISH SOME OFTEN USED CONSTANTS.
  PI = 4.D0 * DATAN(1.D0)
  TWOPI = 2.D0 * PI
  NPR = 2.D0 / 3.D0
  GAMMA = 5.D0 / 3.D0
  RGAS = 8.3143D0 * 1000.0D0 / 4.D0
  CP = 2.5D0 * 8.3143D0 / 4.D0
  KSOLID = 0.16
  SQRI = (1.D0,1.D0) / DSQRT(2.D0)
* GET DETAILS OF THE TAE
  CALL SETVAL
  ARES = PI * RATIO(NUMSEC)**2
* ESTIMATE THE RESONANT FREQUENCY FROM THE LENGTH AND SOUND SPEED DIST.
  LSUM = 0.D0
  OPL = 0.0
  DO 1 J=1,NUMSEC
    LEQUTV = DELEM(J) * POROS(J)
  * LEQUTV = DELEM(J)
  LSUM = LSUM + LEQUTV
  SSPEED = DSQRT(GAMMA * RGAS * TLEFT(J)) * (3.D0 + TRGH(J) / TLEFT(J)) / 4.D0
  1 OPL = OPL + SSPEED * LEQUTV
  F0EST = OPL / (2.D0 * LSUM**2)
* COUNT THE NUMBER OF BINS USED.....
  NUMTOT = 0
  DO 10 J=1,NUMSEC
  10 NUMTOT = NUMTOT + NUMLAY(J)
  NUMTOT = NUMTOT + 1
  FMIN = FREMIN
  FMAX = FREMAX
  NFREQ = NUMFRE
  RETURN
* AMBIENT PRESSURE VARIATION IS HARDWIRED IN HERE
  ENTRY TAE(W,FOFW,FPLUS,PAMBTM)

```

```

PAMB = PAMBTM
* GET THE SPECIFIC ACOUSTIC IMPEDANCE AND PRESSURE AT ALL POINTS.
* START AT THE RIGHT AND MOVE TO THE LEFT.
  IF (TERMIN.EQ.'RIGID') THEN
    CALL VDCHE(TRGH(NUMSEC),PAMB,VISC,DENS(NUMTOT),SSPEED,KGAS)
    CALL ZRIGID(DENS(NUMTOT),SSPEED,VISC,W,Z(NUMTOT))
  ELSE IF (TERMIN.EQ.'FREE') THEN
    CALL VDCHE(TRGH(NUMSEC),PAMB,VISC,DENS(NUMTOT),SSPEED,KGAS)
    CALL GETLAM(DENS(NUMTOT),VISC,W,RATIO(NUMSEC),LAMBDA)
    CALL WNTUBE(LAMBDA,W,SSPEED,K(NUMTOT))
    KA = K(NUMTOT) * RATIO(NUMSEC)
    Z(NUMTOT) = SSPEED * DENS(NUMTOT) * KA * (KA/4.D0 - (0.0D0,0.6D0))
  ELSE IF (TERMIN.EQ.'INFIN') THEN
    CALL VDCHE(TRGH(NUMSEC),PAMB,VISC,DENS(NUMTOT),SSPEED,KGAS)
    CALL GETLAM(DENS(NUMTOT),VISC,W,RATIO(NUMSEC),LAMBDA)
    CALL FTUBE(LAMBDA,FLAM(NUMTOT))
    CALL WNTUBE(LAMBDA,W,SSPEED,K(NUMTOT))
    Z(NUMTOT) = DENS(NUMTOT) * W / (FLAM(NUMTOT) * K(NUMTOT))
  ELSE
    STOP
  END IF
  P1(NUMTOT) = 1.D0
* APPLY THE IMPEDANCE AND PRESSURE TRANSLATION THEOREMS EVERYWHERE.
* WORK FROM RIGHT TO LEFT.
  DO 40 I=NUMSEC,1,-1
    JUP = 0
    DO 50 J=I+1,NUMSEC
50  JUP = JUP + NUMLAY(J)
    JUP = NUMTOT - JUP - 1
    JLOW = JUP - NUMLAY(I) + 1
    DSUB(JUP) = DELEM(I) / NUMLAY(I)
    POROUS(JUP) = POROS(I)
* IMPEDANCE TRANSLATE FOR THE OPEN TUBE OR HEAT EXCHANGER SECTIONS.
    IF (SECTYP(I).EQ.'OPENTU' OR SECTYP(I).EQ.'HEXCH') THEN
      CALL VDCHE(TRGH(I),PAMB,VISC,DENS(JUP),SSPEED,KGAS)
      TAVE(JUP) = TRGH(I)
      TOZ(JUP) = 0.0D0
      ALPHA(JUP) = (0.D0,0.D0)
      CALL GETLAM(DENS(JUP),VISC,W,RATIO(I),LAMBDA)
      LAMBDT = DSQRT(NPR) * LAMBDA
      IF (SECTYP(I).EQ.'OPENTU') THEN
        CALL FTUBE(LAMBDA,FLAM(JUP))
        CALL FTUBE(LAMBDT,FLAMT(JUP))
        CALL WNTUBE(LAMBDA,W,SSPEED,K(JUP))
      * CALL FCYL(LAMBDA,FLAM(JUP))
      * CALL FCYL(LAMBDT,FLAMT(JUP))
      * CALL WNHEX(FLAMT(JUP),FLAM(JUP),W,SSPEED,K(JUP))
    * OTHERWISE, THE TUBE SECTION IS A HEAT EXCHANGER. FIND ITS GEOMETRY.
      ELSE IF (SECTYP(I).EQ.'HEXCH') THEN
        IF (ETYP(I).EQ.'RECT') THEN
          CALL FRECT(ASPECT(I),LAMBDA,FLAM(JUP))
          CALL FRECT(ASPECT(I),LAMBDT,FLAMT(JUP))
        ELSE IF (ETYP(I).EQ.'CYL') THEN
          CALL FCYL(LAMBDA,FLAM(JUP))
          CALL FCYL(LAMBDT,FLAMT(JUP))
        ELSE IF (ETYP(I).EQ.'SLIT') THEN
          CALL FSLIT(LAMBDA,FLAM(JUP))
          CALL FSLIT(LAMBDT,FLAMT(JUP))
        ELSE
          STOP
        * AN ERROR ON THE INPUT OF ETYP(I) HAS OCCURED.
      END IF
      CALL WNHEX(FLAMT(JUP),FLAM(JUP),W,SSPEED,K(JUP))
    END IF
  END IF

```

```

COMDEN(JUP)=DENS(JUP)/FLAM(JUP)
ZINT = COMDEN(JUP) * W / ( K(JUP) * POROUS(JUP) )
AR = K(JUP) * DSUB(JUP)
SN = CDSIN(AR)
CS = CDCOS(AR)
DO 60 J=JUP, JLOW, -1
INSTAK(J)=.FALSE.
DENS(J)=DENS(JUP)
TAVE(J)=TAVE(JUP)
TOZ(J) = TOZ(JUP)
POROUS(J)=POROUS(JUP)
ALPHA(J) = ALPHA(JUP)
FLAM(J) = FLAM(JUP)
FLAMT(J) = FLAMT(JUP)
K(J) = K(JUP)
COMDEN(J) = COMDEN(JUP)
DSUB(J) = DSUB(JUP)
CALL ZPTRAN(ZINT,SN,CS,Z(J+1),Z(J),P1(J+1),P1(J))
60 CONTINUE
ELSE IF (SECTYP(I).EQ.'STACK') THEN
* IMPEDANCE TRANSLATE FOR THE STACK SECTIONS.
TOZ(JUP)=(TRGH(I) - TLEFT(I)) / DELEM(I)
NS = 0
DO 70 J=JUP, JLOW, -1
INSTAK(J)=.TRUE.
NS = NS + 1
TNS = TRGH(I) - (TRGH(I) - TLEFT(I)) * DFLOAT(NS)
* / DFLOAT(NUMLAY(I))
TNSM1 = TRGH(I) - (TRGH(I) - TLEFT(I)) * DFLOAT(NS-1)
* / DFLOAT(NUMLAY(I))
TAVE(J) = (TNS + TNSM1) / 2.D0
POROUS(J) = POROUS(JUP)
DSUB(J) = DSUB(JUP)
TOZ(J) = TOZ(JUP)
* START THE RUNGE-KUTTA
CALL STAKPM(ETYPE(I),W,POROUS(J),PAMB,TNSM1,TOZ(J),DENS(J),
2 RATIO(I),ASPECT(I),FLAM(J),FLAMT(J),ZETA,ALPRIM,ZINT)
CALL DERIVS(ZETA,ZINT,ALPRIM,P1(J+1),Z(J+1),DPDZ,DZDZ)
K1 = -DSUB(J)*DPDZ
M1 = -DSUB(J)*DZDZ
P1(J) = P1(J+1) + K1/2.D0
Z(J) = Z(J+1) + M1/2.D0
CALL STAKPM(ETYPE(I),W,POROUS(J),PAMB,TAVE(J),TOZ(J),DENS(J),
2 RATIO(I),ASPECT(I),FLAM(J),FLAMT(J),ZETA,ALPRIM,ZINT)
CALL DERIVS(ZETA,ZINT,ALPRIM,P1(J),Z(J),DPDZ,DZDZ)
K2 = -DSUB(J)*DPDZ
M2 = -DSUB(J)*DZDZ
P1(J) = P1(J+1) + K2/2.D0
Z(J) = Z(J+1) + M2/2.D0
CALL DERIVS(ZETA,ZINT,ALPRIM,P1(J),Z(J),DPDZ,DZDZ)
K3 = -DSUB(J)*DPDZ
M3 = -DSUB(J)*DZDZ
P1(J) = P1(J+1) + K3
Z(J) = Z(J+1) + M3
CALL STAKPM(ETYPE(I),W,POROUS(J),PAMB,TNS,TOZ(J),DENS(J),
2 RATIO(I),ASPECT(I),FLAM(J),FLAMT(J),ZETA,ALPRIM,ZINT)
CALL DERIVS(ZETA,ZINT,ALPRIM,P1(J),Z(J),DPDZ,DZDZ)
K4 = -DSUB(J)*DPDZ
M4 = -DSUB(J)*DZDZ
P1(J) = P1(J+1) + (K1+2.D0*K2+2.D0*K3+K4)/6.D0
Z(J) = Z(J+1) + (M1+2.D0*M2+2.D0*M3+M4)/6.D0
COMDEN(J)=DENS(J)/FLAM(J)
ALPHA(J) = ALPRIM
70 CONTINUE

```

```

ELSE
* AN ERROR ON INPUT OF SECTYP HAS OCCURED.
STOP
END IF
40 CONTINUE
* THE IMPEDANCE IS NOW KNOWN AT ALL SPOTS IN THE TAE
* GET THE ACOUSTIC PRESSURE, ZCOOR, WORK AND HEAT FLUXES.
* ZCOOR(1) = 0.0D0
IF (TERMIN.EQ.'INFIN') THEN
TFUN = 1.D0 / P1(1)
ELSE
TFUN = (0.D0 - 1.D0) * W * Z(1) * DDRIVE / P1(1)
END IF
! TERMIN.EQ.'INFIN' CONDITIONAL
P1(1) = TFUN * P1(1)
* CALL WFLOW(P1(1),Z(1),W2(1))
DO 80 J=1,NUMTOT-1
P1(J+1) = P1(J+1) * TFUN
* ZCOOR(J+1) = ZCOOR(J) + DSUB(J)
* CALL WFLOW(P1(J+1),Z(J+1),W2(J+1))
* CALL QFLOW(POROUS(J),P1(J),Z(J),FLAM(J),FLAMT(J),W,
* DENS(J),T0Z(J),KGAS,KSOLID,Q2(J))
80 CONTINUE
* J = NUMTOT-1
* CALL QFLOW(POROUS(J),P1(J+1),Z(J+1),FLAM(J),FLAMT(J),W,
* DENS(J),T0Z(J),KGAS,KSOLID,Q2(NUMTOT))
DO 81 J=1,NUMTOT
Q2(J) = Q2(J) * ARES
*81 W2(J) = W2(J) * ARES
* THE SIGN OF Z(1) WAS CHANGED ON 8-12-91. THE IMPEDANCE LOOKING TO
* THE RIGHT HAS TO BE EQUAL TO MINUS THE IMPEDANCE LOOKING TO THE LEFT
* AND THE MINUS SIGN COMES FROM THE DIRECTION OF PARTICLE VELOCITY.
FOFW = SQRI * CDSQRT(DENS(1)**3 * SSPEED**4 * NPR / (W*VISC) /
* (GAMMA - 1.D0) * Z(1))
FPLUS = FOFW - 2.D0 * Z(1)
RETURN
END
*****
* SUBROUTINE CHANGE. USED TO INSERT A NUMBER INTO A LINE OF A
* SEQUENTIAL FILE
*****
SUBROUTINE CHANGE(FNUM,LNUM,TO)
INTEGER FNUM,LNUM,J
CHARACTER*80 LINE
1 FORMAT(A80)
REAL*8 TO
OPEN(3,FILE='SCRATCH')
REWIND(3)
REWIND(FNUM)
DO 10 J=1,5000
READ(FNUM,1,END=20) LINE
IF (J.NE.LNUM) THEN
WRITE(3,1) LINE
ELSE
WRITE(3,*) TO
END IF
10 CONTINUE
20 ENDFILE 3
REWIND(3)
REWIND(FNUM)
DO 30 J=1,5000
READ(3,1,END=40) LINE
30 WRITE(FNUM,1) LINE
40 ENDFILE FNUM
REWIND(3)

```

```

REWIND(FNUM)
RETURN
END

```

- *****
- * PROGRAM : EVALUATE TAE FOR A RANGE OF PARAMETERS.
- * VERSION EXPLICITLY FOR THE UMTAE.
- * PAT ARNOTT, 22 MARCH 1991, MOD 11-15-91.
- * DETERMINES THE STABILITY CURVE FOR THE FIRST TWO MODES AS A FUNCTION
- * OF THE AMBIENT PRESSURE. INCLUDES FINITE WALL POROSITY IN THE STACK.
- *****

```

PROGRAM UMTAE2
* VARIABLES USED TO GET THE Q.
REAL*8 AMPLIT(2000),FREQU(2000),QUAL,RESFRE,RESOLD,QOLD
REAL*8 QOLD2,TOLD2,RSOLD2,TOLD
* VARIABLES RETURNED FROM TAE.
REAL*8 FREMIN,FREMAX,FOEST
INTEGER NUMFRE
* LOCAL VARIABLES TO THE MAINLINE.....
REAL*8 PAMB,PMIN,PMAX,TMIN
REAL*8 TRGH,TONSET,P1,TWOPI,TEST,TESTF,TNOLD,TNOLD2
INTEGER ITRGH,PLOTN,IFREQ,NTIMES,NPAMBS,NPRESS,MODE
COMPLEX*16 W,WNEW,FOFW,DFOFW,FOFWPE,WPEW,EPSIL
COMPLEX*16 FPLUS,DUMB,WMEW,FOFWME,WCOXR,WSTART
* DEFINE THE VARIABLE FOR THE OUTPUT COMMON BLOCK.
PARAMETER (N=5000)
REAL*8 Q2(N),W2(N),ZCOOR(N)
COMPLEX*16 Z(N),P1(N)
LOGICAL INSTAK(N)
COMMON /OUTPUT/ P1,Z,Q2,W2,ZCOOR,INSTAK
* PRELIMINARIES.
PI = 4.D0 * DATAN(1.D0)
TWOPI = 2.D0 * PI
* SET UP THE AMBIENT PRESSURE LOOP.....
PMIN = 2.00D5
PMAX = 8.0D5
PMIN = DSQRT(PMIN)
PMAX = DSQRT(PMAX)
NPAMBS=16
* SET UP THE MODE LOOP.....
DO 18 MODE=2,2
IF (MODE.EQ.2) THEN
TMIN = 603.D0
ELSE
TMIN = 403.D0
END IF
DO 17 NPRESS=14,NPAMBS
WCOXR = (3151.633184D0,-67.8178943D0)/(3152.921237D0,-66.734D0)
PLOTN = 0
QUAL=30.D0
PAMB = PMIN + (PMAX-PMIN) * DFLOAT(NPRESS) / DFLOAT(NPAMBS)
PAMB = PAMB*PAMB
* HOP ON THE TEMPERATURE CALCULATIONS.....
DO 10 ITRGH=INT(TMIN),1593,20
EPSIL = 1.D-8
NTIMES=0
TRGH = DFLOAT(ITRGH)
CALL CHANGE(2,28,TRGH)
CALL CHANGE(2,31,TRGH)
CALL CHANGE(2,36,TRGH)
CALL CHANGE(2,59,TRGH)
CALL CHANGE(2,84,TRGH)
PLOTN = PLOTN + 1
CALL TAE(FREMIN,FREMAX,NUMFRE,FOEST)
FOEST = FOEST*DFLOAT(MODE)

```

```

WRITE (*,111) FOEST
111 FORMAT(' RESONANT FREQUENCY ESTIMATE FROM OPL ',F9.3)
* IF (PLOTN.NE.1) FREMIN = RESFRE*(1.D0 - 0.5D0 / QUAL)
* START THE COMPLEX EIGENFREQUENCY ALGORITHM WITH THE DRIVEN SYSTEM Q.
IF ((QUAL.LT.200.D0).AND.((QUAL.GT.0.D0).AND.(PLOTN.LT.7))) THEN
DO 100 IFREQ=1,NUMFRE
IF (NUMFRE.EQ.1) THEN
FREQ = FREMIN
ELSE
FREQ = FREMIN + (FREMAX-FREMIN)*DFLOAT(IFREQ)/DFLOAT(NUMFRE-1)
END IF
FREQ=FREQ*DFLOAT(MODE)
W = TWOPI * FREQ
CALL TAE1(W,POFW,FPLUS,PAMB)
AMPLIT(IFREQ)=CDABS(P1(1))
100 FREQ(IFREQ) = FREQ
* GET THE Q AND RESONANT FREQUENCY USING THE CONSTANT AMPLIT DRIVER
* RESPONSE
CALL QUAFAC(AMPLIT,FREQ,QUAL,RESFRE)
WRITE (29,1010) RESFRE,QUAL,TRGH-293.D0
WRITE (27,*) TRGH-293.D0,1.D0/QUAL
WRITE (28,*) TRGH-293.D0,RESFRE
WRITE (*,1010) RESFRE,QUAL,TRGH-293.D0
1010 FORMAT(' ROTE: RES FREQ=',F9.3, ' Q=',F9.3, ' DELTAT=',F9.3, ' K')
ELSE ! LINEARLY INTERPOLATE TO GET A START FOR QUAL AND RESFRE.
* 1/QUAL AND RESFRE ARE ASSUMED TO BE LINEAR IN DELTA T.
QUAL=1.D0*QOLD+(QOLD-QOLD2)*(TRGH-TOLD)/(TOLD2-TOLD)*QOLD2*QOLD)
QUAL = 1.D0 / QUAL
RESFRE= RESOLD + (RSOLD2-RESOLD)*(TRGH-TOLD)/(TOLD2-TOLD)
END IF ! THIS ENDS THE INITIAL SEARCH FOR A START Q AND RESFRE.
* NOW GET THE COMPLEX EIGENFREQUENCY FOR COMPARISON.
* INITIAL GUESS FOR THE NEWTON'S TECHNIQUE OF ROOT DETERMINATION.
W = TWOPI * RESFRE * (1.D0 - (0.D0,0.5D0)/QUAL)
WSTART = W
IF (((MODE.EQ.2).AND.(PLOTN.NE.1)).OR.(MODE.EQ.1)) W = W * W CORR
WRITE (*,*) DREAL(W)/TWOPI,DREAL(W)/(2.D0*DIMAG(W))
110 CALL TAE1(W,POFW,FPLUS,PAMB)
NTIMES=NTIMES+1
WPEW = W * (1.D0 + EPSIL)
WMEW = W * (1.D0 - EPSIL)
CALL TAE1(WPEW,POFWPE,DUMB,PAMB)
CALL TAE1(WMEW,POFWME,DUMB,PAMB)
DPOFW = (POFWPE - POWFME) / (2.D0 * EPSIL)
WNEW = W - 100.D0 * POWF / DPOFW
EPSIL = (WNEW - W)*2.D-4/(WNEW+W)
* TEST = CDABS((WNEW-W)/(WNEW+W))
TESTF = CDABS(POFW/FPLUS)
* IF ((TEST.GT.1.D-4).OR.(TESTF.GT.1.D-4)) THEN
IF (TESTF.GT.1.D-5) THEN
W = WNEW
GOTO 110
ELSE ! COMPLEX EIGENFREQUENCY HAS BEEN FOUND.
W = (W + WNEW) / 2.D0
W CORR = W / WSTART
WRITE (*,*) NTIMES
WRITE (*,*) POWF
END IF ! TEST.GT. OR TESTF.GT. CONDITIONAL
* GET THE Q AND RESONANT FREQUENCY.
RESFRE = DREAL(W) / TWOPI
QUAL = -DREAL(W)/(2.D0 * DIMAG(W))
WRITE (39,1011) RESFRE,QUAL,TRGH-293.D0,PAMB
WRITE (37,*) TRGH-293.D0,1.D0/QUAL
WRITE (38,*) TRGH-293.D0,RESFRE
WRITE (*,1011) RESFRE,QUAL,TRGH-293.D0,PAMB

```

```

1011 FORMAT(' EIG: F0,F9.3, Q,F9.3, DT,F9.3, K', PAMB,F10.2)
* DETERMINE IF ONSET HAS BEEN ACHIEVED: IF SO, GET DT AND RESFRE, NEXTP
  IF (PLOTN.EQ. 1) THEN
    RESOLD = RESFRE
    QOLD = QUAL
    TOLD = TRGH
  ELSE
    IF (QOLD*QUAL.LT. 0.D0) THEN
      INTERPOLATE TO GET THE ONSET DELTA T.
      TONSET = TOLD + (TRGH - TOLD)*(1.D0 - QOLD/QUAL)
      WRITE (44,*) PAMB,TONSET-293.D0,MODE
      WRITE (*,1117) PAMB,TONSET-293.D0,MODE
1117 FORMAT(' AMBIENT PRES ',F10.2,' ONSET DELTAT',F9.3,' MODE',I3)
      GOTO 17
    ELSE
      ! RESET OLD PARAMETERS TO NEW PARAMETERS.
      RSOLD2 = RESOLD
      QOLD2 = QOLD
      TOLD2 = TOLD
      RESOLD = RESFRE
      QOLD = QUAL
      TOLD = TRGH
    END IF
  END IF
  ! ONSET CONDITIONAL
  ! PLOTN.EQ. 1
10 CONTINUE
  ! TEMPERATURE LOOP INCREMENT
  TNOLD2=TNOLD
  TNOLD=TONSET
17 CONTINUE
  ! PRESSURE LOOP INCREMENT
18 CONTINUE
  ! MODE LOOP INCREMENT
  END

```

MAINLINE USED TO COMPUTE THE RESONANT FREQUENCY AND QUALITY FACTOR CURVES.

- PROGRAM : EVALUATE TAE FOR A RANGE OF PARAMETERS.
- VERSION EXPLICITLY FOR THE UMTAE
- PAT ARNOTT, 22 MARCH 1991, MOD 11-15-91.
- DETERMINES THE STABILITY CURVE FOR THE FIRST TWO MODES AS A FUNCTION
- OF THE AMBIENT PRESSURE. INCLUDES FINITE WALL POROSITY IN THE STACK.
- PROGRAM USED TO DETERMINE THE Q AND RESFRE OF THE UMTAE VS TEMPERATURE

```

PROGRAM UMTAE2
* VARIABLES USED TO GET THE Q.
REAL*8 AMPLT(2000),FREQ(2000),QUAL,RESFRE,RESOLD,QOLD
REAL*8 QOLD2,TOLD2,RSOLD2,TOLD
* VARIABLES RETURNED FROM TAE
REAL*8 FREMIN,FREMAX,FOEST
INTEGER NUMFRE
* LOCAL VARIABLES TO THE MAINLINE.....
REAL*8 PAMB,PMIN,PMAX,TMIN
REAL*8 TRGH,TONSET,PI,TWOPI,TEST,TESTF,TNOLD,TNOLD2
INTEGER ITRGH,PLOTN,IFREQ,NTIMES,NPAMBS,NPRESS,MODE
COMPLEX*16 W,WNEW,FOFW,DFOFW,FOFWPE,WPEW,EPSIL
COMPLEX*16 FPLUS,DUMB,WMEW,FOFWME,WCORR,WSTART
* DEFINE THE VARIABLE FOR THE OUTPUT COMMON BLOCK
PARAMETER (N=5000)
REAL*8 Q2(N),W2(N),ZCOOR(N)
COMPLEX*16 Z(N),P1(N)
LOGICAL INSTAK(N)
COMMON /OUTPUT/ P1,Z,Q2,W2,ZCOOR,INSTAK
* PRELIMINARIES.
PI = 4.D0 * DATAN(1.D0)
TWOPI = 2.D0 * PI
* SET UP THE AMBIENT PRESSURE LOOP.....
PMIN = 1.73D5
PMAX = 1.73D5

```



```

TMIN = 293.D0
NPAMBS = 1
• SET UP THE MODE LOOP.....
DO 18 MODE = 2,2
DO 17 NPRESS = 1, NPAMBS
  W CORR = (3151.633184D0, -67.8178943D0) / (3152.921237D0, -66.734D0)
  PLOTN = 0
  QUAL = 30.D0
  PAMB = PMIN + (PMAX - PMIN) * DFLOAT(NPRESS) / DFLOAT(NPAMBS)
• HOP ON THE TEMPERATURE CALCULATIONS.....
DO 10 ITRGH = INT(TMIN), 1593, 20
  EPSIL = 1.D-8
  NTIMES = 0
  TRGH = DFLOAT(ITRGH)
  CALL CHANGE(2,28,TRGH)
  CALL CHANGE(2,31,TRGH)
  CALL CHANGE(2,56,TRGH)
  CALL CHANGE(2,59,TRGH)
  CALL CHANGE(2,84,TRGH)
  PLOTN = PLOTN + 1
  CALL TAE(FREMIN, FREMAX, NUMFRE, FOEST)
  FOEST = FOEST * DFLOAT(MODE)
  WRITE (*,111) FOEST
111  FORMAT(' RESONANT FREQUENCY ESTIMATE FROM OPL ',F9.3)
• IF (PLOTN.NE.1) FREMIN = RESFRE * (1.D0 - 0.5D0 / QUAL)
• START THE COMPLEX EIGENFREQUENCY ALGORITHM WITH THE DRIVEN SYSTEM Q.
  IF ((QUAL.LT.200.D0).AND.(QUAL.GT.0.D0)) THEN
    DO 100 IFREQ = 1, NUMFRE
    IF (NUMFRE.EQ.1) THEN
      FREQ = FREMIN
    ELSE
      FREQ = FREMIN + (FREMAX - FREMIN) * DFLOAT(IFREQ) / DFLOAT(NUMFRE-1)
    END IF
    FREQ = FREQ * DFLOAT(MODE)
    W = TWOPI * FREQ
    CALL TAE1(W, FOFW, FPLUS, PAMB)
    AMPLT(IFREQ) = CDABS(P1(1))
100  FREQ(IFREQ) = FREQ
• GET THE Q AND RESONANT FREQUENCY USING THE CONSTANT AMPLT DRIVER
• RESPONSE
  CALL QUAFAC(AMPLT, FREQ, QUAL, RESFRE)
  WRITE (29,1010) RESFRE, QUAL, TRGH-293.D0
  WRITE (27,*) TRGH-293.D0, 1.D0/QUAL, MODE
  WRITE (28,*) TRGH-293.D0, RESFRE, MODE
  WRITE (*,1010) RESFRE, QUAL, TRGH-293.D0
1010  FORMAT(' ROTE: RES FREQ=',F9.3, ' Q=',F9.3, ' DELTAT=',F9.3, ' K')
  ELSE ! LINEARLY INTERPOLATE TO GET A START FOR QUAL AND RESFRE
• 1/QUAL AND RESFRE ARE ASSUMED TO BE LINEAR IN DELTA T.
  QUAL = 1.D0/QOLD - (QOLD-QOLD2) * (TRGH-TOLD) / (TOLD2-TOLD) * QOLD2/QOLD
  QUAL = 1.D0/QUAL
  RESFRE = RESOLD + (RSOLD2-RESOLD) * (TRGH-TOLD) / (TOLD2-TOLD)
  END IF ! THIS ENDS THE INITIAL SEARCH FOR A START Q AND RESFRE
• NOW GET THE COMPLEX EIGENFREQUENCY FOR COMPARISON.
• INITIAL GUESS FOR THE NEWTON'S TECHNIQUE OF ROOT DETERMINATION.
  IF ((MODE.EQ.2).AND.((QUAL.GT.100.D0).OR.(QUAL.LT.0.D0)))
    • THEN ! THE ROUTINE IS OK FOR THE HIGHER MODE.... GO AHEAD
    W = TWOPI * RESFRE * (1.D0 - (0.D0, 0.5D0)/QUAL)
    WSTART = W
    IF ((MODE.EQ.2).AND.(PLOTN.NE.1)).OR.(MODE.EQ.1)) W = W * W CORR
    WRITE (*,*) DREAL(W)/TWOPI, DREAL(W)/(2.D0*DIMAG(W))
110  CALL TAE1(W, FOFW, FPLUS, PAMB)
    NTIMES = NTIMES + 1
    WPEW = W * (1.D0 + EPSIL)
    WMEW = W * (1.D0 - EPSIL)

```

```

CALL TAE1(WPEW,FOFWPE,DUMB,PAMB)
CALL TAE1(WMEW,FOFWME,DUMB,PAMB)
DFOFW = (FOFWPE - FOFWME) / (2.D0 * EPSIL)
WNEW = W - 100.D0 * FOFW / DFOFW
EPSIL = (WNEW - W) ^ 2.D-4 / (WNEW + W)
* TEST = CDABS(WNEW-W) / (WNEW+W)
TESTF = CDABS(FOFW/FPLUS)
* IF ((TEST.GT. 1.D-4) .OR. (TESTF.GT. 1.D-4)) THEN
IF (TESTF.GT. 1.D-5) THEN
W = WNEW
GOTO 110
ELSE
! COMPLEX EIGENFREQUENCY HAS BEEN FOUND.
W = (W + WNEW) / 2.D0
WCORR = W / WSTART
WRITE (*,*) NTIMES
WRITE (*,*) FOFW
END IF
! TEST.GT. OR TESTF.GT. CONDITIONAL
* GET THE Q AND RESONANT FREQUENCY.
RESFRE = DREAL(W) / TWOPI
QUAL = -DREAL(W) / (2.D0 * DIMAG(W))
WRITE (39,1011) RESFRE,QUAL,TRGH-293.D0,PAMB
WRITE (37,*) TRGH-293.D0,1.D0,QUAL,MODE
WRITE (38,*) TRGH-293.D0,RESFRE,MODE
WRITE (*,1011) RESFRE,QUAL,TRGH-293.D0,PAMB
1011 FORMAT(' EIG: F0',F9.3,' Q',F9.3,' DT',F9.3,' K:',PAMB,F10.2)
* DETERMINE IF ONSET HAS BEEN ACHIEVED: IF SO, GET DT AND RESFRE, NEXTP
IF (PLOTN.EQ. 1) THEN
RESOLD = RESFRE
QOLD = QUAL
TOLD = TRGH
ELSE
IF (QOLD*QUAL.LT. 0.D0) THEN
* INTERPOLATE TO GET THE ONSET DELTA T.
TONSET = TOLD + (TRGH - TOLD) / (1.D0 - QOLD/QUAL)
WRITE (44,*) PAMB,TONSET-293.D0,MODE
WRITE (*,1117) PAMB,TONSET-293.D0,MODE
*1117 FORMAT(' AMBIENT PRES ',F10.2,' ONSET DELTAT',F9.3,' MODE',B)
GOTO 17
ELSE
! RESET OLD PARAMETERS TO NEW PARAMETERS.
RSOLD2 = RESOLD
QOLD2 = QOLD
TOLD2 = TOLD
RESOLD = RESFRE
QOLD = QUAL
TOLD = TRGH
END IF
! ONSET CONDITIONAL
END IF
! PLOTN.EQ. 1
END IF
! CONDITIONAL ON MODE.EQ.2 AND Q>100.
10 CONTINUE
! TEMPERATURE LOOP INCREMENT
TNOLD2=TNOLD
TNOLD=TONSET
17 CONTINUE
! PRESSURE LOOP INCREMENT
18 CONTINUE
! MODE LOOP INCREMENT
END

```

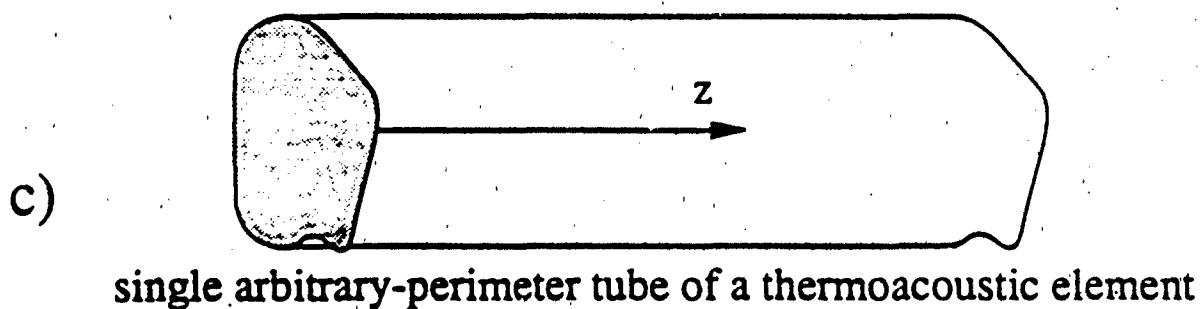
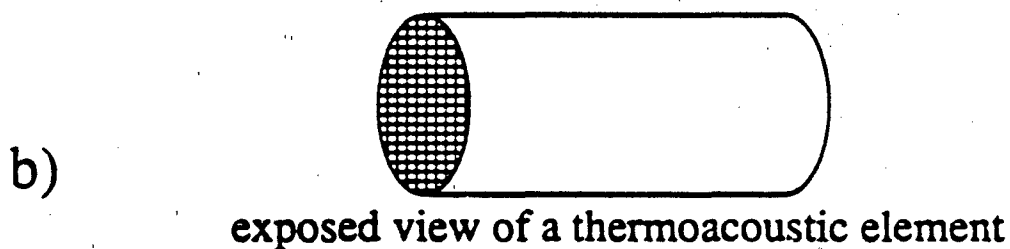
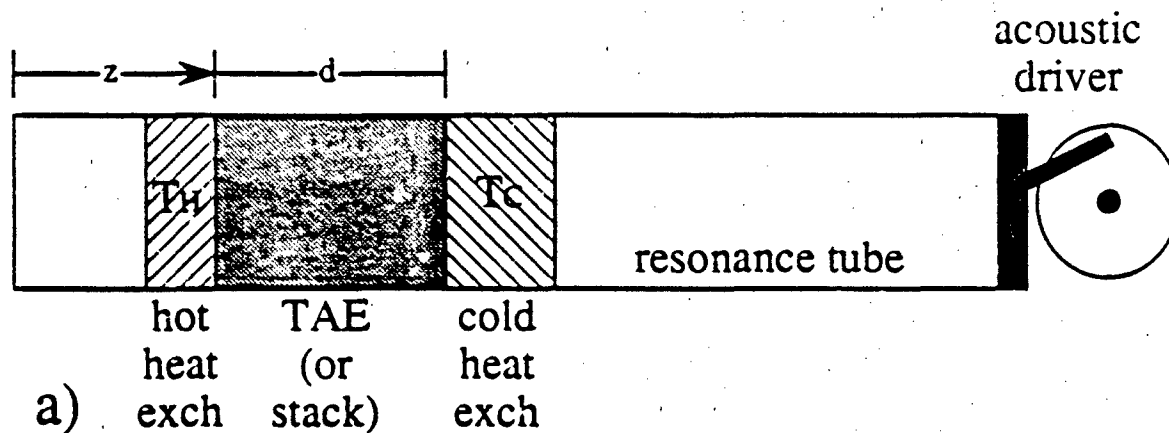


Figure 1. a) Generic arrangement used in thermoacoustic heat engines. b) An exposed view of a thermoacoustic element consisting of a parallel combination of square capillary tubes. c) A single arbitrary-perimeter capillary tube for use in a thermoacoustic element.

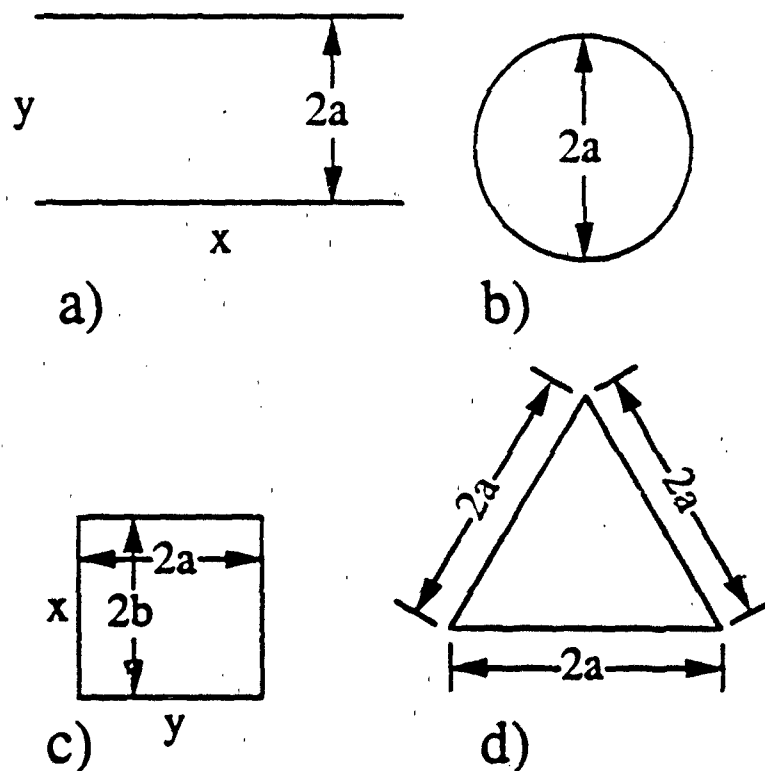


Figure 2. a) Parallel plate, b) circular, c) rectangular, and d) equilateral triangular capillary tube geometries

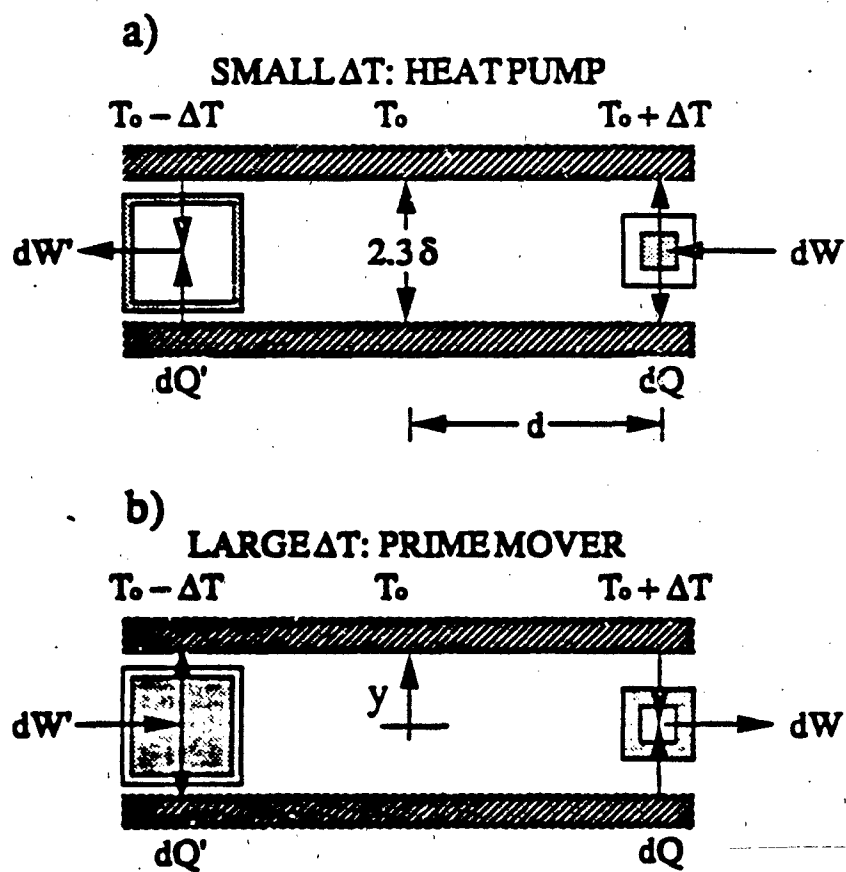


Figure 3. Lagrangian view of a fluid parcel in a standing wave near a boundary.

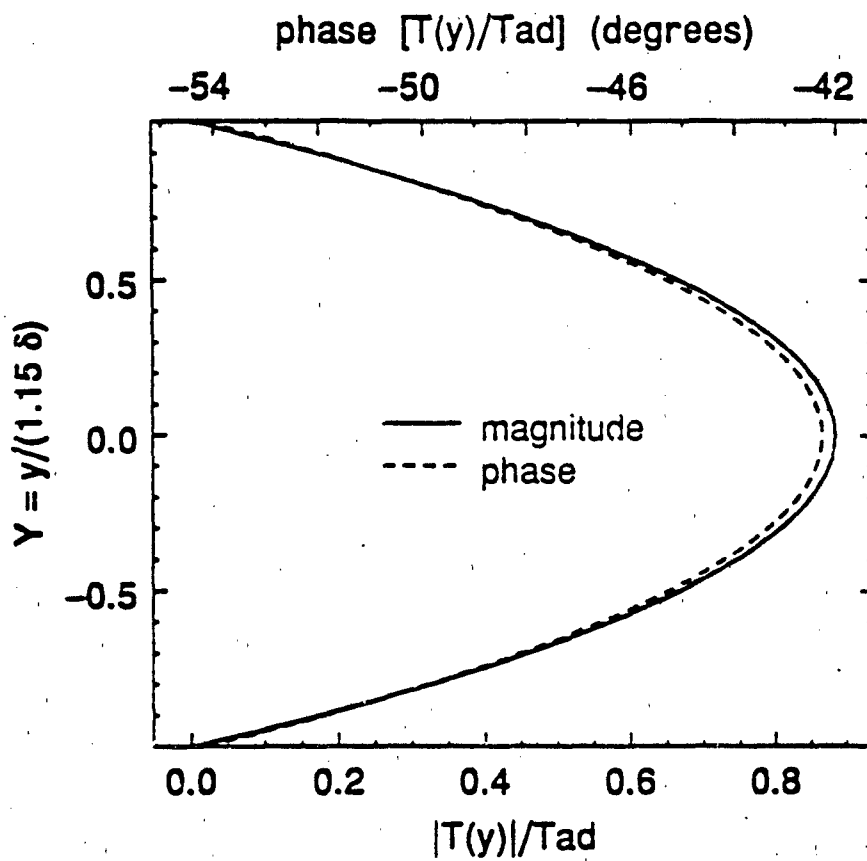


Figure 4. Magnitude and phase of the excess temperature between parallel plates.

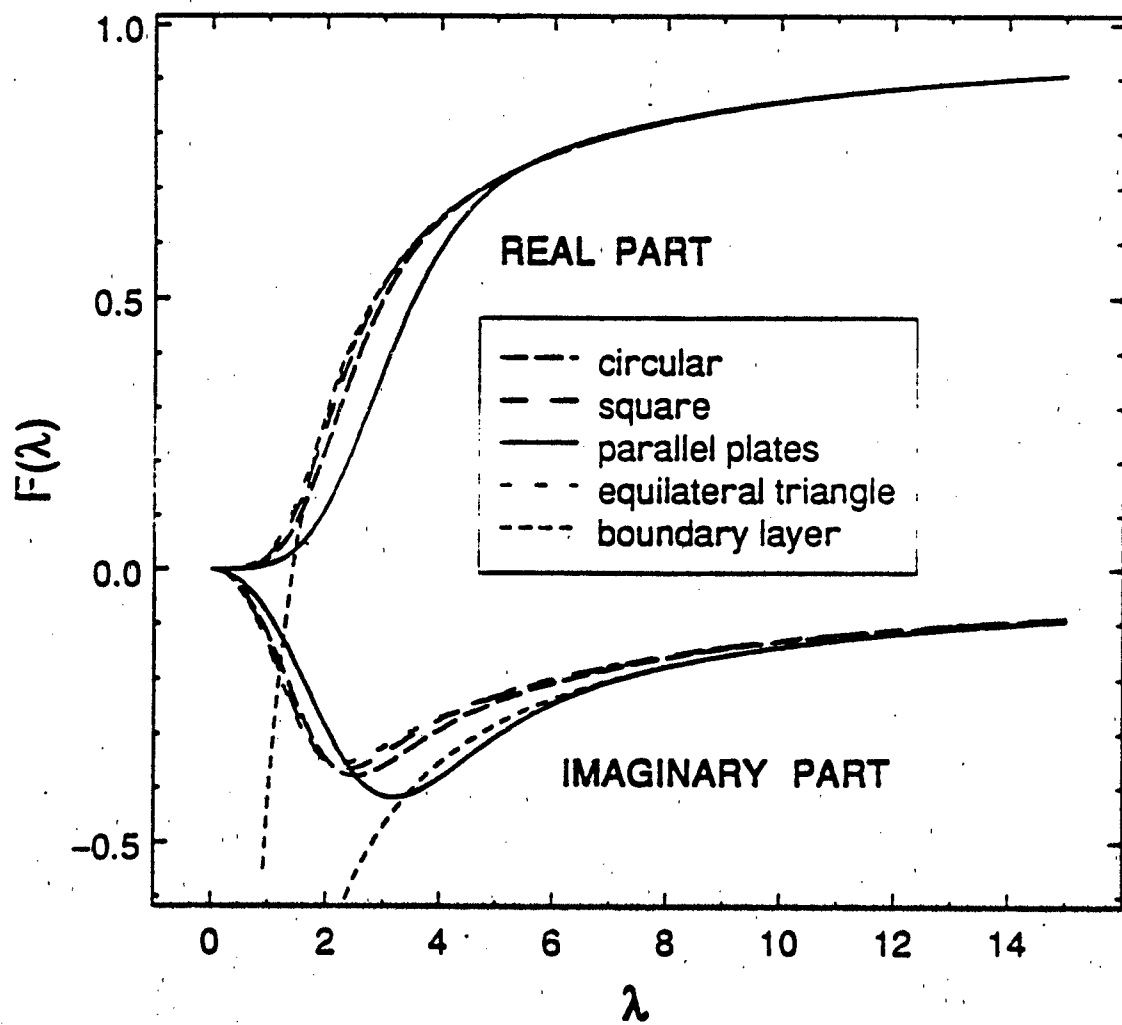


Figure 5. Real and Imaginary part of the $F(\lambda)$ different pore geometries.

THERMOACOUSTIC PRIME MOVER

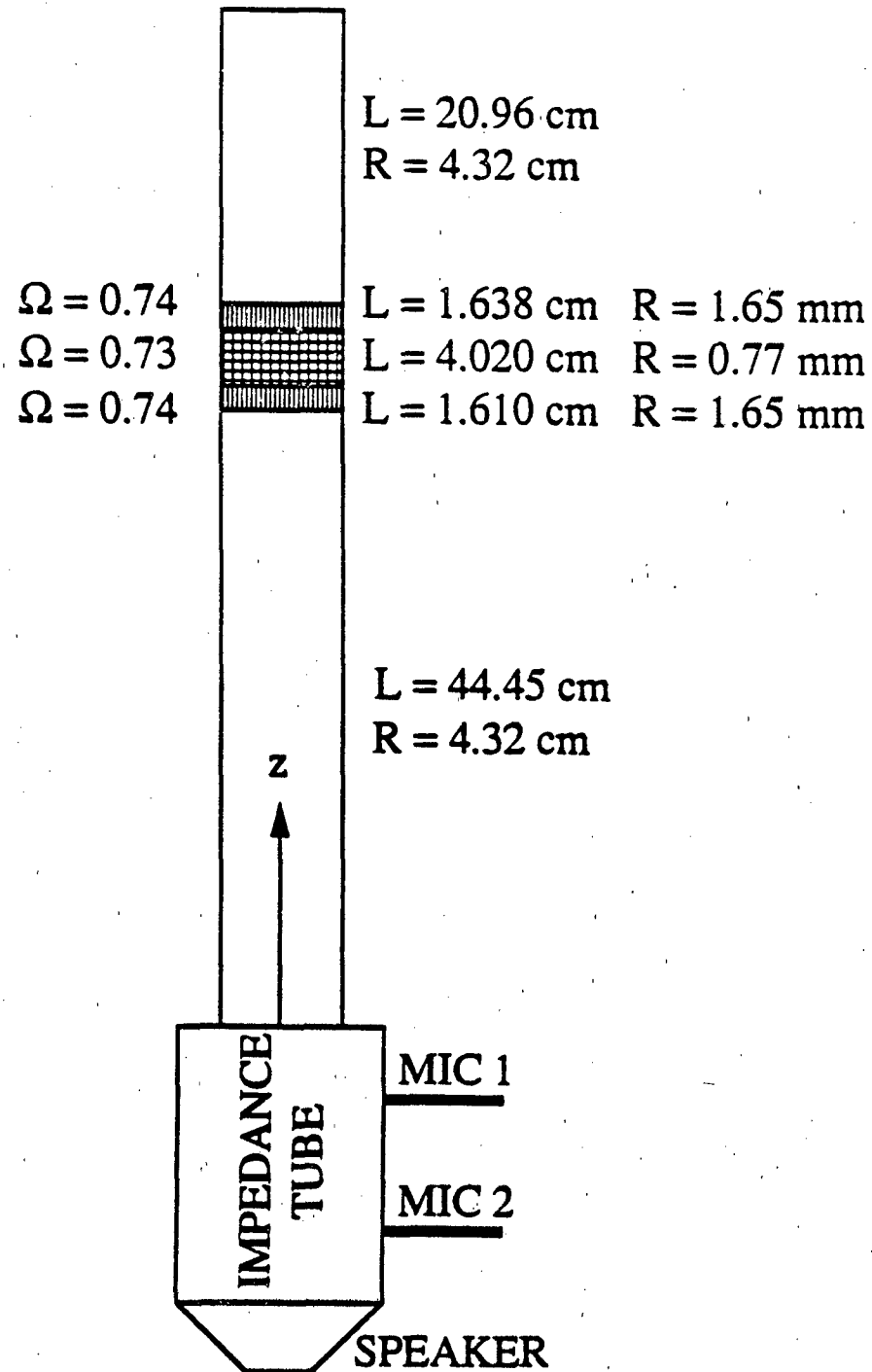


Figure 6. Demonstration thermoacoustic oscillator and analysis impedance tube.

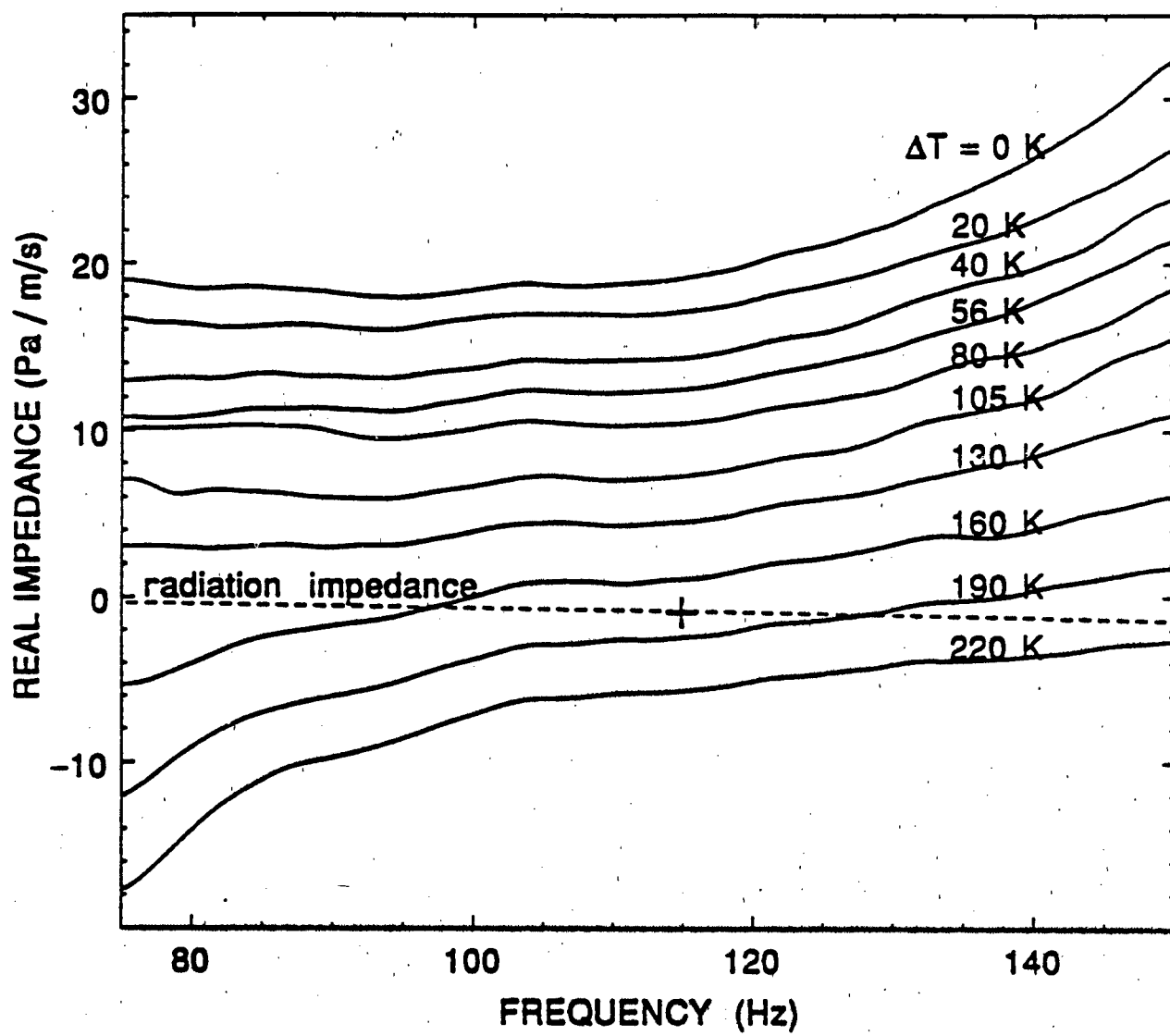


Figure 7. Real part of the specific acoustic impedance at the mouth of the prime mover.

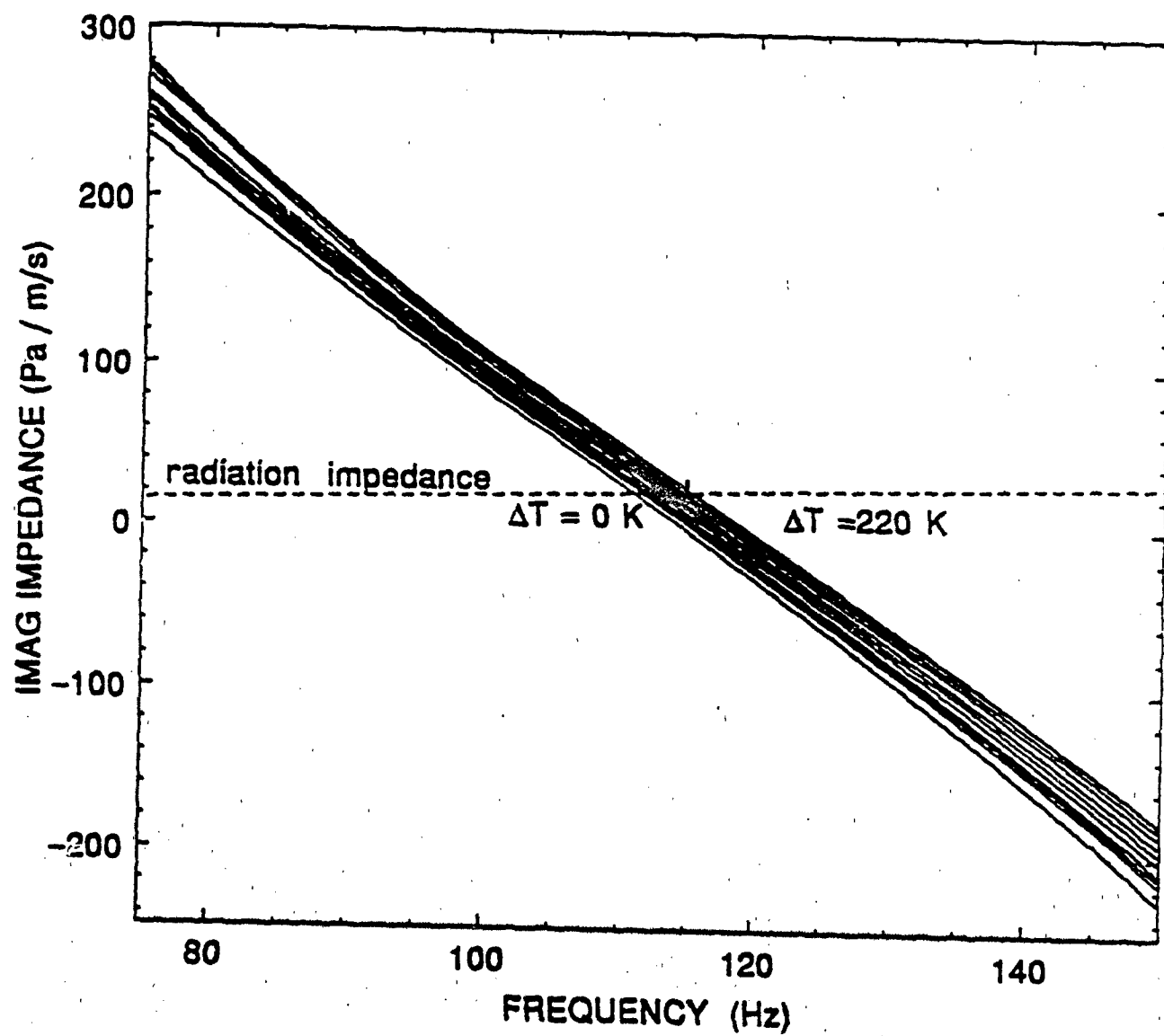


Figure 8. Imaginary part of the specific acoustic impedance.

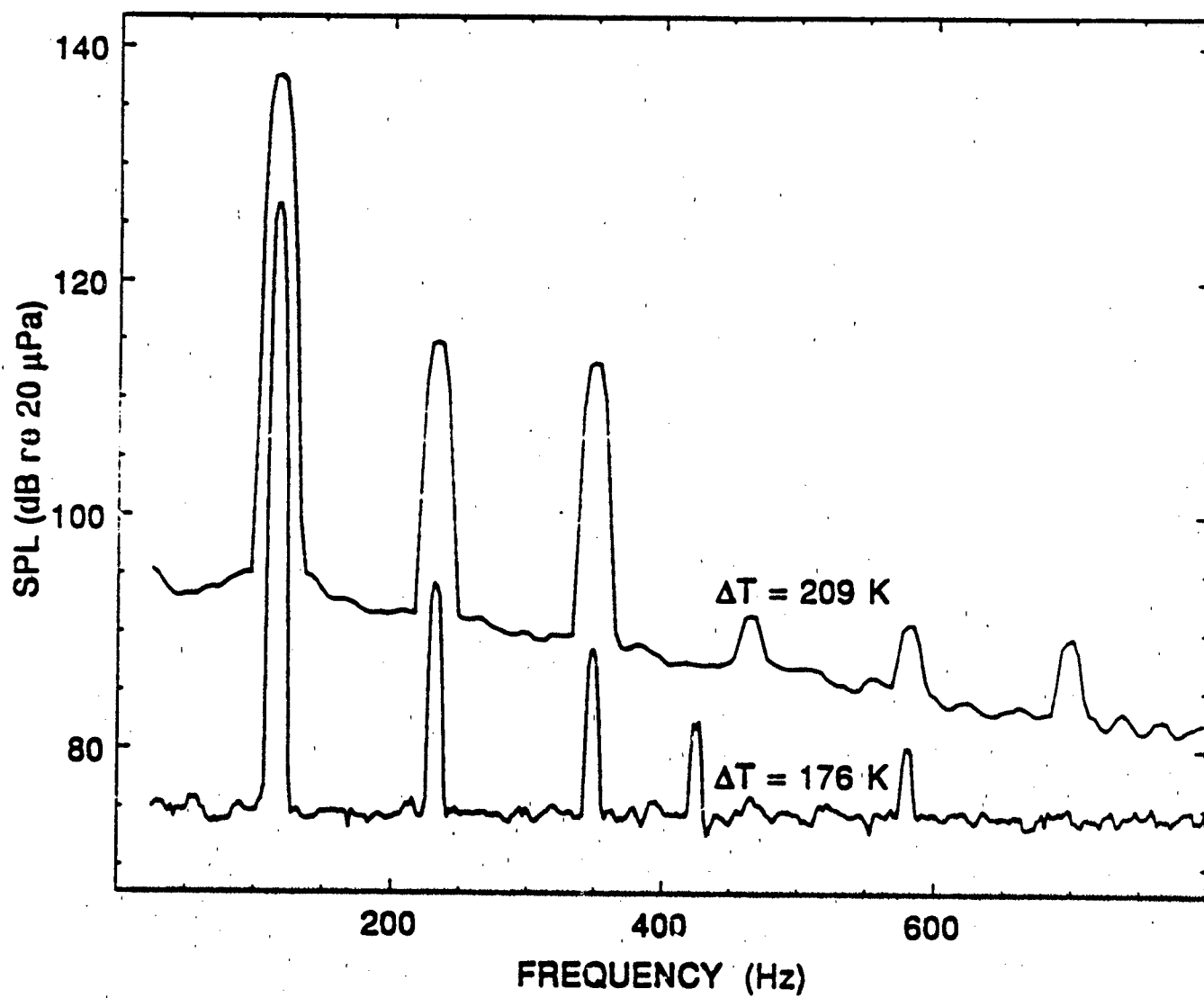


Figure 9. Prime mover sound spectrum for onset $\Delta T = 176$ K and a higher $\Delta T = 209$ K.

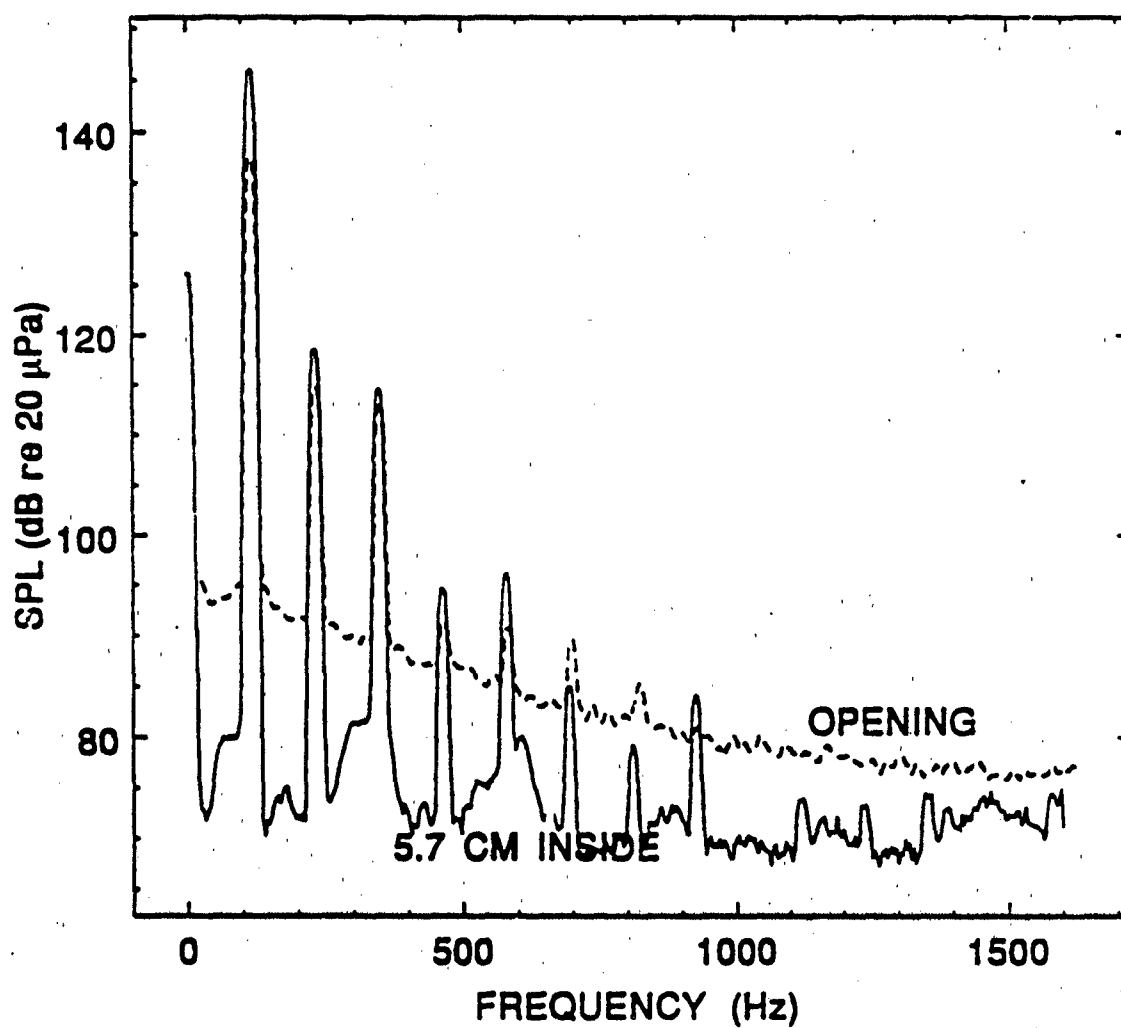


Figure 10. Prime mover sound spectrum for $\Delta T = 209$ K in mouth, 5.7 cm inside prime mover.

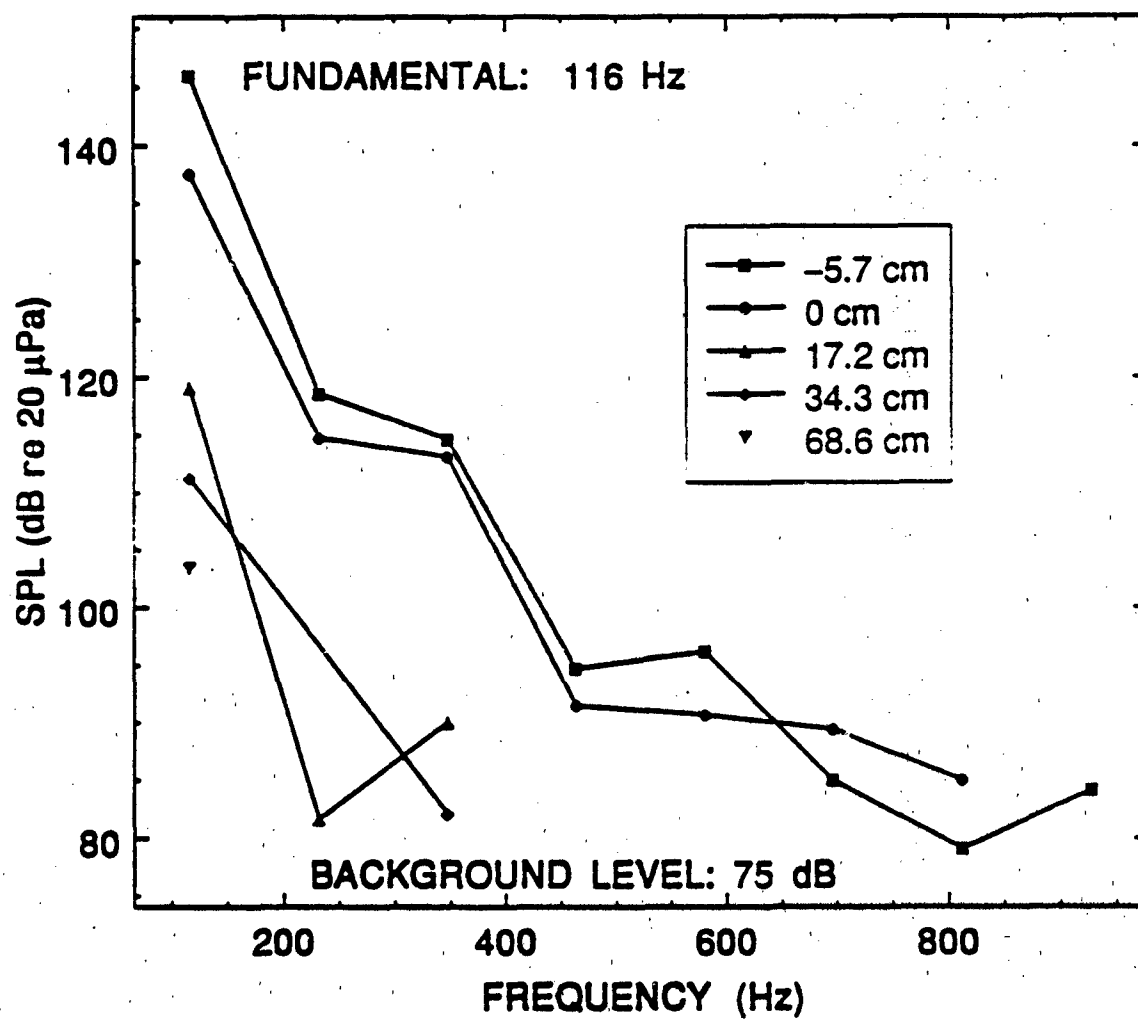


Figure 11. Spectral peaks as a function of distance from the mouth of the prime mover.

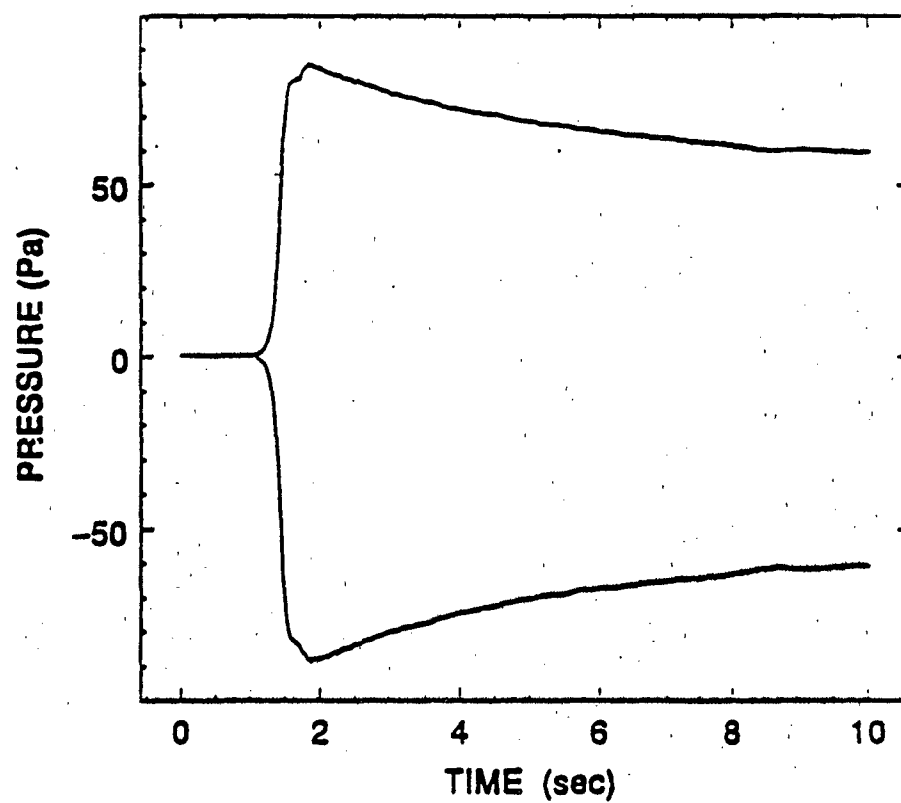
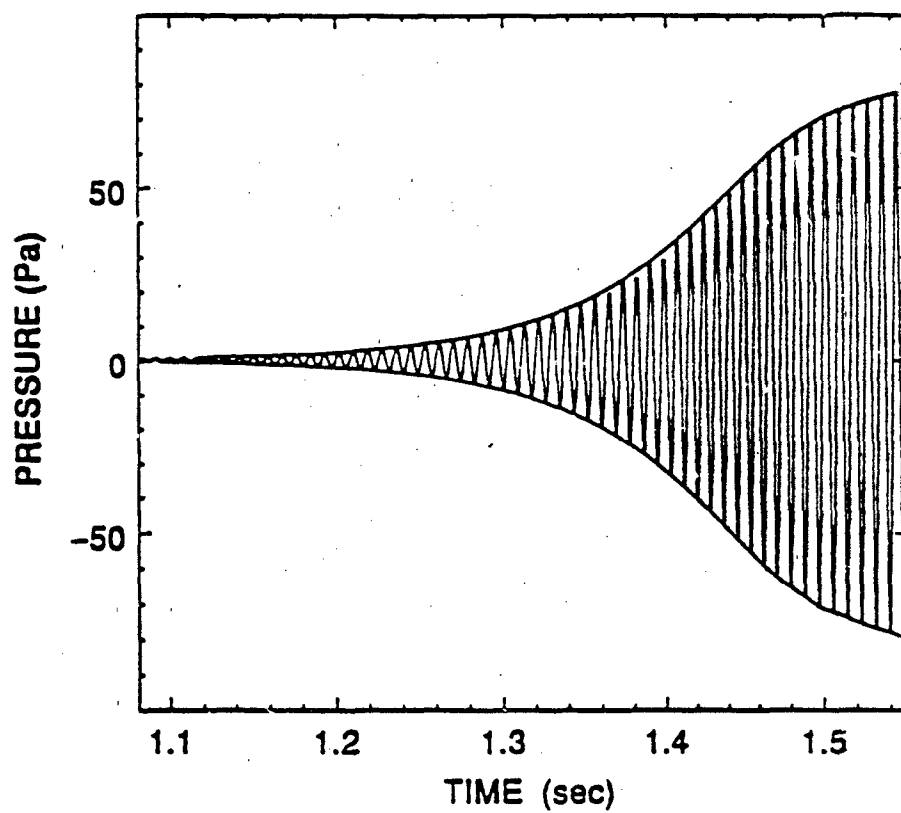


Figure 12. Time evolution of the superheated prime mover.

SCALE DRAWING OF UM TAE:

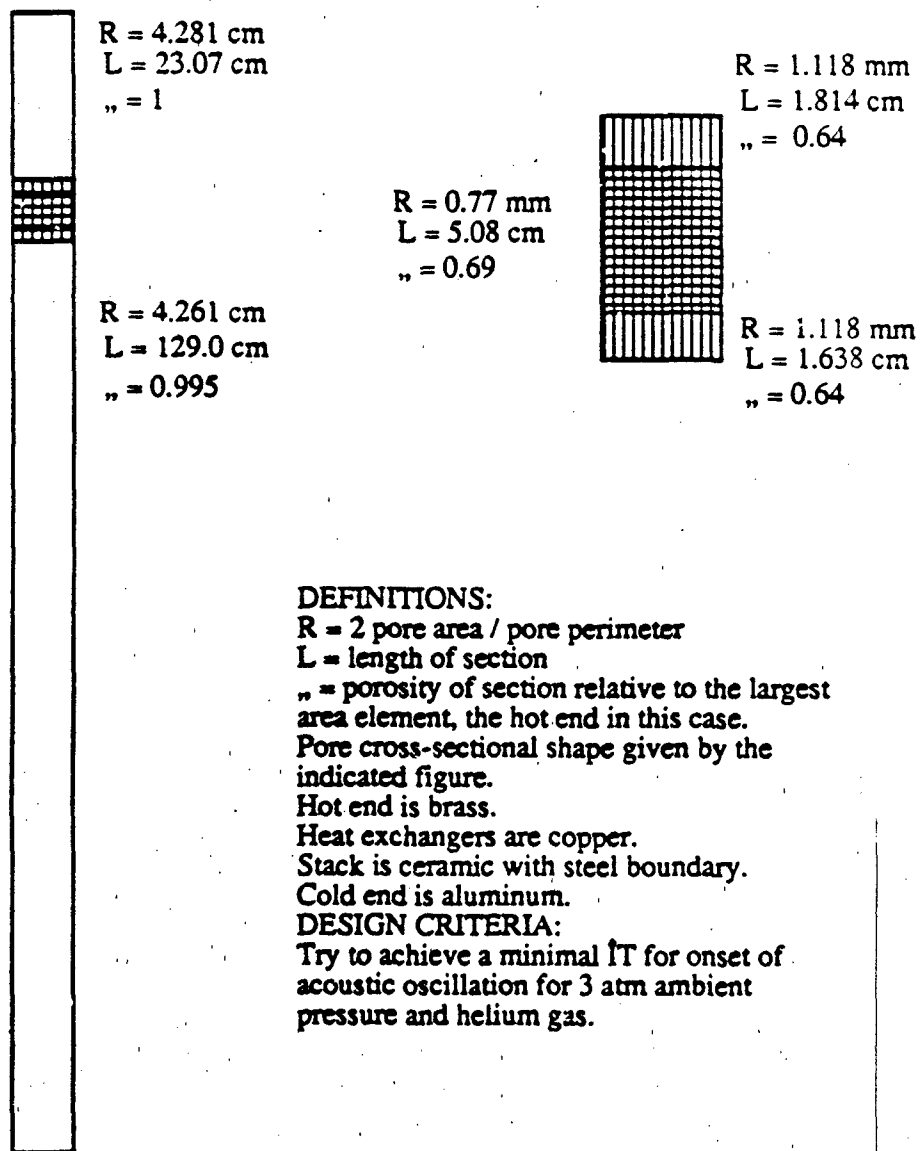


Figure 13. Scale drawing for the fundamental and first harmonic for the UM TAE.

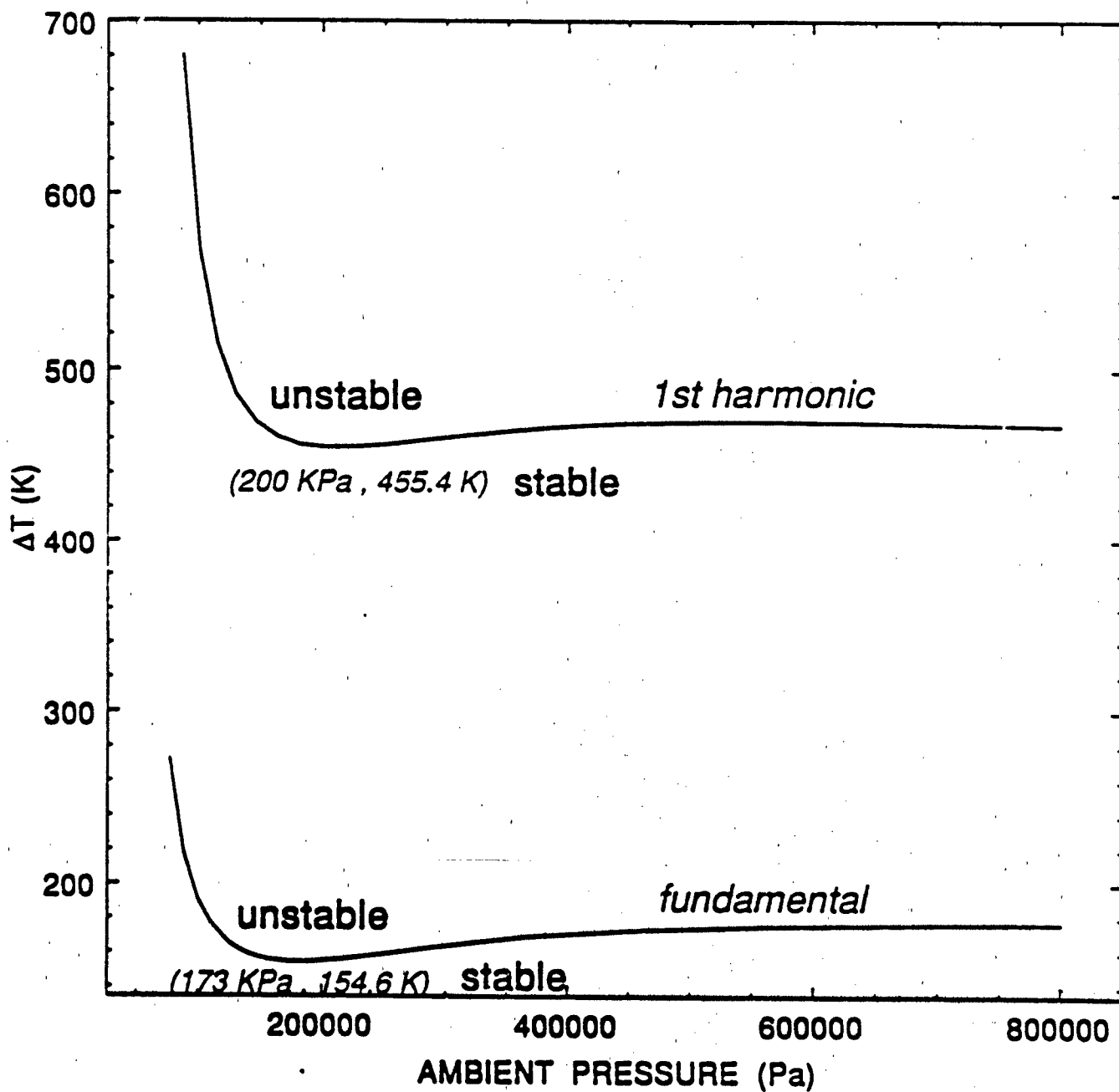


Figure 14. Stability curves for the fundamental and first harmonic for the UM TAE.

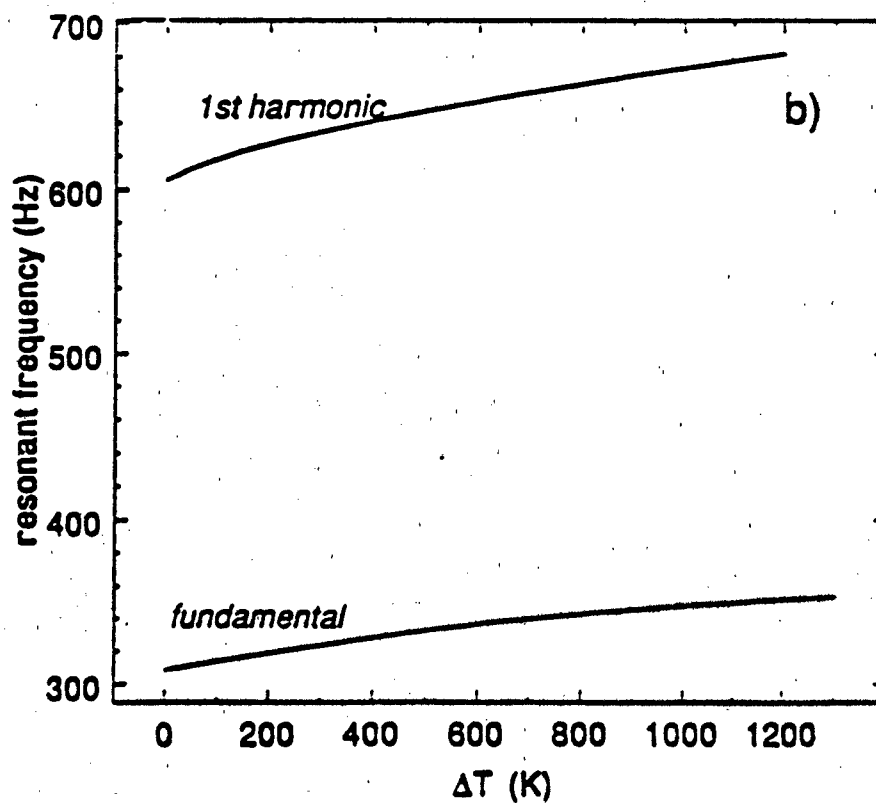
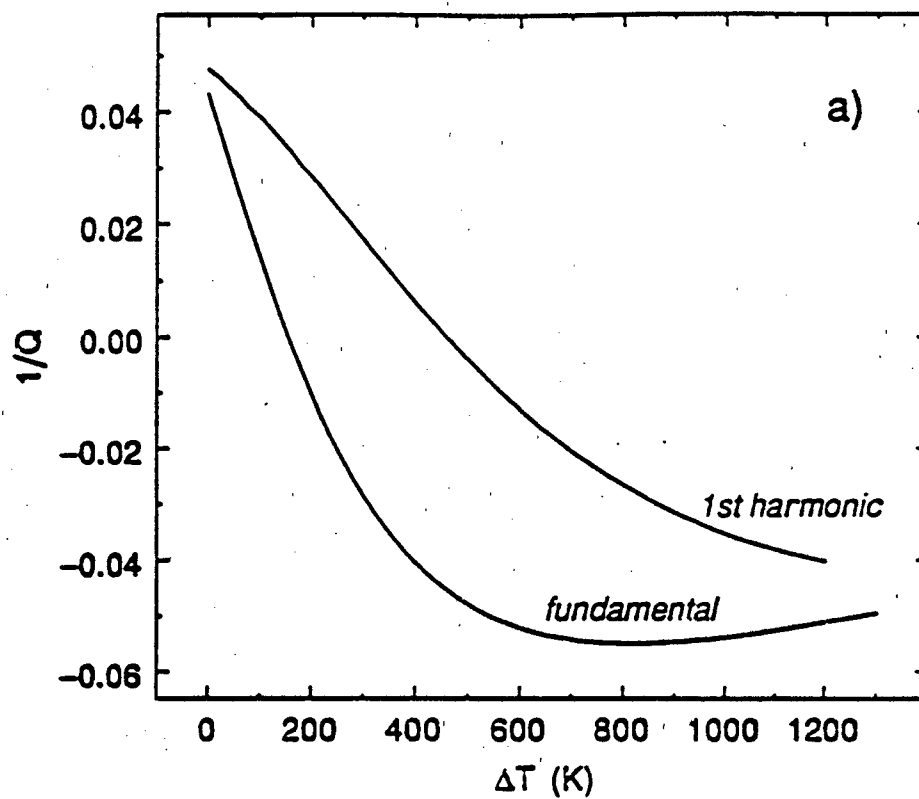


Figure 15. a) Quality factor, b) resonant frequency for UM TAE with ambient pressure 173 kPa.

**END
FILMED**

DATE:

3-92

DTIC